The Empirical Performance of the Financial Accelerator since 2008

Gregor Boehl[a,*], Felix Strobel[b]

[a] *University of Bonn*
[b] *Deutsche Bundesbank*

April 16, 2023

Abstract

We evaluate the empirical performance of financial frictions à la Bernanke et al. (1999) during and after the Global Financial Crisis. We document that in an ex-post analysis based on nonlinear Bayesian methods, these frictions do not improve the standard medium-scale DSGE model's ability to explain the macroeconomic dynamics during the Great Recession. The reason is that in the estimated model with financial frictions, the drastic post-2008 collapse of investment causes firms' leverage to decline. Taking the model at face value, this would trigger a narrowing of the credit spread, contradicting the observed persistently large credit spread troughout the post-2008 period. Additionally, the estimated model attributes only a minor role to the associated financial shocks. These findings are confirmed independently for US and euro area data.

Keywords: Financial Frictions, Great Recession, Business Cycles, Effective Lower Bound, Nonlinear Bayesian Estimation
JEL: C11, C63, E31, E32, E44

⋆Some of the content of this paper was previously circulating as part of a draft with the title "US Business Cycle Dynamics at the ZLB". We are grateful to Christian Bayer, Pavel Brendler, Flora Budianto, Alex Clymo, Macro Del Negro, Simon Gilchrist, Gavin Goy, Joachim Jungherr, Alexander Meyer-Gohde, Daniel Rees, Alexander Richter, Mathias Trabandt, Carlos Zarazaga and participants of the 2018 Stanford MMCI Conference, the 2018 EEA Annual Congress, the 2018 VfS Jahrestagung and a seminar at the Deutsche Bundesbank for discussions and helpful comments on the contents of this paper. The views expressed in this paper are solely the responsibility of the authors and should not be interpreted as reflecting the views of the Deutsche Bundesbank. Part of the research leading to the results in this paper has received financial support from the Alfred P. Sloan Foundation under the grant agreement G-2016-7176 for the MMCI at the IMFS Frankfurt. Gregor Boehl gratefully acknowledges the financial support provided by the Deutsche Forschungsgemeinschaft (DFG) under CRC-TR 224 (projects C01 and C05) and under project number 441540692.

*Corresponding author. Address: Institute for Macroeconomics and Econometrics, University of Bonn, Adenauerallee 24-42, 53113 Bonn, Germany

Email address: gboehl@uni-bonn.de

1 Introduction

The Global Financial Crisis and the subsequent Great Recession spurred the interest of academics and policy makers in understanding the inter-linkages between the financial sector and business cycles. Consequently, the literature on financial frictions in structural macroeconomic models has become one of the most active in the field of macroeconomics. Within this literature, one of the most prominent frameworks is the seminal financial accelerator model of Bernanke et al. (1999, BGG).

In the model, an agency problem between lenders and borrowing firms motivates an external finance premium that is tied to the firms' leverage. Since the firms' financial positions depend on the macroeconomic environment, the model creates an elegant link between business cycle fluctuations and credit market conditions. In turn, endogenous developments in the credit market work to amplify and propagate shocks to the macroeconomy. Thus, the framework provides researchers with a convenient tool to investigate the connection between the surging financial spreads in the Global Financial Crisis and the subsequent Great Recession, and has consequently found widespread use in central banks and academia.[1]

We pursue a very simple strategy to evaluate the empirical performance of BGG's financial accelerator with the benefit of hindsight: We first use nonlinear Bayesian methods to estimate a medium-scale DSGE model with financial accelerator on macroeconomic data which spans broadly over the great recession. We then compare the marginal data density of the estimated model to that of an estimated model without financial accelerator. As the marginal data density is a very rigorous, yet transparent measure of empirical fit it yields a natural and generic device for scientific hypothesis testing. Any proposed modelling extension should be able to outperform the baseline model.

As the model with a financial accelerator, we employ the framework by Del Negro et al. (2015), who develop a medium-scale model with a financial sector in the vein of BGG. An advantage of their model is that switching off the financial friction results in the canonical medium-scale representative agent New Keynesian ("RANK") model of Smets and Wouters (2007), which is conveniently nested. Using the estimated RANK model as a benchmark and comparing it with the full estimated model with the financial sector ("FRANK") allows us to test for the ex-post explanatory power of financial frictions á la BGG of the post-2008 US macroeconomic dynamics. To overcome the challenge of the long-lasting binding effective lower bound on nominal interest rates (ELB), we employ the novel set of estimation methods developed in Boehl and Strobel (2022).

[1] Among many others, examples for studies that build on this framework are Christensen and Dib (2008); De Graeve (2008); Darracq Pariès et al. (2011); Brzoza-Brzezina and Kolasa (2013); Del Negro and Schorfheide (2013); Verona et al. (2013); Christiano et al. (2014); Del Negro et al. (2015); Carlstrom et al. (2016); Rannenberg (2016); Villa (2016); Zivanovic (2019).

Our central finding is that the canonical RANK model without financial frictions outperforms the FRANK model with BGG's financial accelerator both in term of the empirical fit and in terms of providing a parsimonious account of the Great Recession. By construction, the difference between the two models is that in FRANK, the credit spread (the difference between the return on capital and the risk-free rate) is tied to firms' leverage. A higher leverage raises the credit spread. However, we show that while the leverage ratio increases in the estimated model during the crisis, it falls substantially thereafter and stays below its pre-crisis level for the remainder of our sample, which ends in 2019:IV. This deleveraging is due to the substantial decline in the capital stock that is implied by the collapse of investment in the Great Recession, and actually causes the model-implied spread to *fall*.

This implication is at odds with the empirical evidence. In the data, the credit spread remained above its pre-crisis level for a protracted time after its initial spike at the onset of the financial crisis. That suggests that the extraordinary crisis left scars in the US financial system that resulted in a *financial hysteresis*. As we document, the estimated FRANK model does not generate this phenomenon endogenously. Instead, to match the prolonged period of elevated spreads in the data, the lower model-implied credit spread in the estimated model must be compensated by additional financial shocks. This worsens the empirical performance of the full FRANK model compared to the RANK model.

We document further that through the mechanism outlined above, the introduction of a financial sector attenuates the decline in investment in response to recessionary shocks. This is problematic because after 2008, the considerable decline in investment was a key feature of both the US and the Euro Area economy. In the estimated FRANK model, the collapse of investment in the Great Recession causes a decline in the leverage ratio. This reduces the required return on investment, thereby dampening the overall fall in investment: the financial accelerator becomes a *financial attenuator*. Hence, the addition of the financial sector impedes the ability of the model to explain the characteristics of this episode. We show that this issue applies to recessionary risk premium shocks as well as for shocks to the marginal efficiency of investment, both of which have previously been identified as the main drivers of the Great Recession (e.g. Del Negro and Schorfheide, 2013; Christiano et al., 2015).

To ensure a clean comparison, we estimate the FRANK model and its RANK counterpart on the same set of time series, including the time series of the credit spread. As RANK lacks a role for a spread, we assume that the spread data is purely driven by an exogenous AR(1) process, which does not affect the macroeconomic dynamics in the RANK model. In the FRANK model, the credit spread is endogenously determined by the financial friction additional to a financial shock. Importantly, we would expect that this additional modeling feature would partly explain the dynamics of the spread data, and thereby reduce the need for additional exogenous shocks.

This, in turn, should improve the empirical fit of the model. Yet, we find that this is not the case in practice. Rather, the endogenous propagation *including* the financial shock is outperformed by the AR(1) process.

Our analysis suggests that through the lens of the RANK model elevated risk premiums in household financing are the dominant driver of the crisis and have a large explanatory power for the joint movement of consumption and investment thereafter. This shock can either be interpreted as an economy-wide increase in the demand for liquid or safe assets (Fisher, 2015), or it can be associated with the importance of household financing for the Great Recession. This latter interpretation analysis corroborates the work by Mian and Sufi (2014, 2015) and Guerrieri and Lorenzoni (2017), and is in line with Kehoe et al. (2020), who argue that the credit tightening for households contributed more to the downturn than the credit tightening for firms. In FRANK, however, as the financial attenuator effect reduces the explanatory power of risk premium shocks for investment dynamics, investment is mostly driven by shocks to the marginal efficiency of investment. Thus, FRANK explains consumption and investment with two disparate drivers.

In the estimated FRANK model, risk shocks as in Christiano et al. (2014) play only a minor role for the macroeconomic dynamics. As these shocks are inflationary and hence put upwards pressure on the policy rate via the Taylor rule, a more prominent role of these shocks would be hard to reconcile with the prolonged binding of the ELB. Our results are consistent with the finding by Christiano et al. (2014), who show that the explanatory power of the risk shock hinges on the inclusion of a broad set of financial variables in the set of observables on which the model is estimated. In contrast to their work, the focus of this paper is to empirically test the explanatory power of BGG's financial accelerator for *macroeconomic* dynamics, and we thus estimate our models largely on macroeconomic variables. Using more observables in the estimation would risk that the likelihood is dominated by non-macroeconomic variables. We further document that it is not straightforward to select the approriate financial quantities. As we show in Appendix D, several plausible candidates exist, which each imply quite different paths for the aggregate US leverage ratio.

Repeating our estimations for euro area data, we show that the financial accelerator falls short of improving the explanation of the events on the other side of the Atlantic as well. The unfolding of the financial crisis and the response of monetary policy differed in many important aspects in the euro area. Notably, the ECB steered the deposit facility rate into negative territory. Yet despite these differences, the poor performance of the financial accelerator is common to both settings. As in the US, the introduction of the accelerator reduces the importance of the risk premium shock and attributes the recession to various different shocks instead of offering a unifying narrative. Again, the role of financial shocks for business cycle dynamics is minor. At the same time, our results for the US economy are also robust to employing shorter samples that have a narrower focus on the

Great Recession.

Related literature

Our analysis is related to Brzoza-Brzezina and Kolasa (2013), who show that the inclusion of BGG-type frictions in a small-scale New Keynesian model does not improve its empirical fit on US data.[2] We go beyond their analysis in several dimensions. Whereas their sample ends early on in the financial crisis and they do not capture the effects of the ELB, we also evaluate the performance of the financial accelerator in the long-lasting aftermath of the financial crisis when the ELB was binding. This allows us to highlight that the observed financial hysteresis phenomenon of persistently high credit spreads in the Great Recession is not compatible with the decline in the leverage ratio, as it is implied by the model. Thereby, we provide a comprehensive rationale for the lower empirical fit of the financial accelerator model.

Whereas the financial accelerator as in BGG's does not enhance the RANK model's empirical fit, a branch of the literature documents that it does improve upon the model's forecasting performance. In the context of the Great Recession this is shown by Del Negro and Schorfheide (2013); Del Negro et al. (2015) and Cai et al. (2019). The FRANK model's advantage is that the introduction of financial frictions allows for a model-consistent role of financial spreads for macroeconomic dynamics. As financial data are available earlier than national account data and at a higher frequency, this benefits out-of-sample forecasts, in particular, during a financial crisis. However, as we show, it does not necessarily enhance the ex-post explanation of the data.

By including post-2008 data in our estimations, we extend prominent contributions in the literature, which analyze the Great Recession and the ELB period through the lens of models that have been calibrated to or estimated on pre-crisis data (see, e.g., Gertler and Karadi, 2011; Christiano et al., 2014, 2015; Del Negro et al., 2015; Carlstrom et al., 2017). As our analysis suggests – and illustrated by Boehl and Strobel (2022) and Boehl et al. (forthcoming) – the post-2008 part of the data sample carries important information that significantly shapes the respective parameter estimates.

To render the analysis of the empirical performance of financial frictions with post-2008 data possible, we employ the novel set of Bayesian methods introduced in Boehl and Strobel (2022). This allows us to account for the binding ELB on nominal interest rates in the estimation procedure. Accordingly, we use the method of Boehl (2022a) to solve for the ELB as an occasionally binding constraint, which grants a significant increase in computational speed compared to alternative algorithms. The Bayesian filter for the likelihood inference of the nonlinear model is an adapted version of Evensen (1994, 2009). Furthermore, to allow us to quickly sample from pos-

[2] Additionally, they also find that frictions as in Kiyotaki and Moore (1997) reduce the fit of the model.

sibly multi-modal high-dimensional posterior distributions *in parallel*, we apply the DIME Monte Carlo Markov Chain method suggested by Boehl (2022b). Boehl and Strobel (2022) further suggest a method to compute historic shock decompositions of linearized models with occasionally binding constraints. Notably, the results of this method are independent of the ordering of shocks, and do not require elaborated sampling and simulation schemes.

We proceed as follows: Section 2 briefly sketches the baseline RANK model and the FRANK extension. Section 3 introduces the methodology as well as the data used. Section 4 briefly discusses the parameter estimates, presents estimates of quantitative measures of the model fit, and provides interpretations of the Great Recession through the lens of the estimated models. Section 5 discusses the mechanisms behind the relatively poor performance of the FRANK model relative to RANK. Section 6 extends our results to the euro area. Section 7 concludes.

2 Models

In our analysis, we employ two models. We use the canonical medium-scale framework by Smets and Wouters (2007) as a baseline. In addition, we present an extended model, which includes financial frictions in the vein of Bernanke et al. (1999) to gauge their role in explaining the Great Recession. We dub the model that includes only a representative agent the *RANK* model. The model vintage including financial frictions will be referred to as the financial representative agent NK model – *FRANK*.

2.1 Baseline model - RANK

We adopt the framework of (Smets and Wouters, 2007, SW) as a baseline model to interpret the Great Recession. Deviating from SW, and following Del Negro and Schorfheide (2013), we detrend all nonstationary variables by

$$Z_t = e^{\gamma t + \frac{1}{1-\alpha}\widetilde{z}_t}, \tag{1}$$

where, γ is the steady-state growth rate of the economy and α is the output share of capital. $\widetilde{z}_t$ is the linearly detrended log productivity process that follows the autoregressive law of motion $\widetilde{z}_t = \rho_z \widetilde{z}_{t-1} + \sigma_z \epsilon_z$. For z_t, the growth rate of technology in deviations from γ, it holds that $z_t = \frac{1}{1-\alpha}(\rho_z - 1)\widetilde{z}_t + \frac{1}{1-\alpha}\sigma_z \epsilon_z$.

We take into account the fact that the central bank is constrained in its interest rate policy by a lower bound (ELB) on the nominal interest rate, r_t. Therefore, in the linear model, it holds that

$$r_t = \max\{\bar{r}, r_t^n\}, \tag{2}$$

with $\bar{r}$ being the lower bound value. Whenever the policy rate is away from the constraint, it corresponds to the notional rate, r_t^n, which follows a conventional feedback rule

$$r_t^n = \rho r_{t-1}^n + (1-\rho)\left(\phi_\pi \pi_t + \phi_y \widetilde{y}_t\right) + \phi_{dy}\Delta\widetilde{y}_t + v_{r,t}, \tag{3}$$

where $\widetilde{y}_t$ is the output gap and $\Delta\widetilde{y}_t = \widetilde{y}_t - \widetilde{y}_{t-1}$ its growth rate. Parameter ρ expresses an interest rate smoothing motive by the central bank. ϕ_π, ϕ_y and ϕ_{dy} are feedback coefficients. $v_{r,t}$ is governed by an exogenous AR(1) process.

As the model is well established, we direct the reader to Appendix C for the full set of linearized equilibrium conditions.

2.2 Model with Financial Frictions - FRANK

The extended model includes frictions in financial markets. We adopt the modeling choices by Del Negro et al. (2015), who build on the work of Bernanke et al. (1999), De Graeve (2008) and Christiano et al. (2014). Entrepreneurs obtain loans from frictionless intermediaries, which in turn receive their funds from household at the riskless interest rate. In addition to the loans, entrepreneurs use their own net worth to finance the purchase of physical capital, which they rent out to intermediate good producers. They are subject to idiosyncratic shocks to their ability to manage capital. As a consequence, their revenue might fall short of the amount needed to repay the loan, in which case they will default on their loan. In anticipation of the risk of entrepreneurs' default, financial intermediates pool their loans and charge a spread on the riskless rate to cover the expected losses arising from defaulting entrepreneurs. Crucially, the spread of the loan rate $\widetilde{r}_t^k$ over the risk free nominal interest rate, r_t, depends on the entrepreneurial leverage and can be written as

$$E_t[\widetilde{r}_{t+1}^k - r_t] = u_t + \zeta_{sp,b}(q_t + \overline{k}_t - n_t) + \widetilde{\sigma}_{\omega,t}. \tag{4}$$

Here, u_t is the risk premium shock on the housholds' borrrowing rate, q_t is the price of capital, $\overline{k}_t$ is the capital stock and n_t denotes entrepreneurial net worth. $\widetilde{\sigma}_{\omega,t}$ is a shock to the entrepreneurs' riskiness and follows an AR(1) process – the risk shock introduced by Christiano et al. (2014). Thus, the loan spread is defined as a function of the entrepreneurs' leverage and their riskiness, which is determined by the dispersion of the idiosyncratic shocks to entrepreneurs. The real loan rate is linked to the return on capital by

$$\widetilde{r}_t^k - \pi_t = \frac{r^k}{r^k + (1-\delta)} r_t^k + \frac{(1-\delta)}{r^k + (1-\delta)} q_t - q_{t-1}, \tag{5}$$

where π_t is the inflation rate, r_t^k and r^k denote the dynamics and the steady state of the marginal product of capital, and parameter δ is the depreciation rate. Note that if the elasticity of the loan

rate to the entrepreneurs' leverage, $\zeta_{sp,b}$, is set to zero we are back to the case without financial frictions. The left hand side of Equation 5 would then read $(r_{t-1} - \pi_t + u_{t-1})$ as in the Smets and Wouters (2007) model. The parameter is eventually estimated.

The evolution of aggregate entrepreneurial net worth is described by

$$n_t = \zeta_{n,\bar{r}^k}(\bar{r}^k_t - \pi_t) - \zeta_{n,r}(r_{t-1} - \pi_t) + \zeta_{n,qk}(q_{t-1} + \bar{k}_{t-1}) + \zeta_{n,n} n_{t-1} - \frac{\zeta_{n,\sigma_\omega}}{\zeta_{sp,\sigma_\omega}} \widetilde{\sigma}_{\omega,t-1} - \gamma_* \frac{v_*}{n_*} \widetilde{z}_t. \tag{6}$$

Equation (6) links the accumulated stock of entrepreneurial net worth to the real return of renting out capital to firms, the riskless real rate, its capital holdings, its past net worth and variations in riskiness. The technology process enters the equation due to the form of detrending we borrow from Del Negro et al. (2015). Likewise, the coefficients $\zeta_{n,\bar{r}^k}$, $\zeta_{n,r}$, $\zeta_{n,qk}$, ζ_{n,σ_ω}, ζ_{sp,σ_ω}, γ_*, v_* and n_* are derived as in Del Negro et al. (2015).

3 Methodology and Data

Data samples in which the ELB is binding pose a host of technical challenges for the estimation of DSGE models. These are related to the solution, likelihood inference, and posterior sampling of models in the presence of an occasionally binding constraint (OBC). While methods to solve models with OBCs exist, and – likewise – nonlinear filters are available, the combination of both is computationally very expensive for medium-scale models. In this section, we briefly summarize the set of novel methods that allow us to conduct the estimation of medium-scale models in the presence of an occasionally binding ELB.[3] Secondly, we discuss our choices with regard to the data, calibrated parameters, and priors used in the empirical analysis.

3.1 Solution method

Throughout this paper, we apply the solution method for DSGE models with OBCs that is presented in Boehl (2022a). We refer to the original paper for details. The model is linearized around its steady state balanced growth path and thereby implicitly detrended. Respecting the ELB, the original model with variable vector $y_t \in \mathbb{R}^{n_y}$ and shock vector $\varepsilon_t \in \mathbb{R}^{n_z}$ can be represented as a piecewise linear model with

$$A \begin{bmatrix} c_t \\ s_{t-1} \end{bmatrix} + b \max \left\{ p \begin{bmatrix} E_t c_{t+1} \\ s_t \end{bmatrix} + m \begin{bmatrix} c_t \\ s_{t-1} \end{bmatrix}, \bar{r} \right\} = E_t \begin{bmatrix} c_{t+1} \\ s_t \end{bmatrix}, \tag{7}$$

[3]The Python-implementation of the tools used for our analysis is freely available at `https://github.com/gboehl/pydsge`.

where $\begin{bmatrix} c_t \\ s_{t-1} \end{bmatrix}$ is a re-ordering of $\begin{bmatrix} y_t \\ \varepsilon_t \end{bmatrix}$: s_{t-1} contains all the (latent) state variables and the current shocks, and c_t contains all forward looking variables. A is the system matrix and $\bar{r}$ is the minimum value of the constrained variable r_t (which is the nominal interest rate for our purpose). The constraint is included with $r_t = \max\left\{ pE_t \begin{bmatrix} c_{t+1} \\ s_t \end{bmatrix} + m \begin{bmatrix} c_t \\ s_{t-1} \end{bmatrix}, \bar{r} \right\}$. p and m measure how r_t is affected by other variables, and the vector b contains the effects of r_t onto all other variables. Then, denote by $(k, l) \in \mathbb{N}_0^+$ the expected duration of the ELB spell and the expected number of periods before the ELB binds.

It can be shown that the rational expectations solution to Equation (7) for the state s periods ahead, (c_{t+s}, s_{t+s-1}), can be expressed in terms of s_{t-1} and the expectations on k and l as

$$F_s(l, k, s_{t-1}) = A^{\max\{s-l,0\}} \hat{A}^{\min\{l,s\}} \begin{bmatrix} f(l, k, s_{t-1}) \\ s_{t-1} \end{bmatrix} + (I - A)^{-1} \left(I - A^{\max\{s-l,0\}} \right) b\bar{r}, \tag{8}$$

$$= E_t \begin{bmatrix} c_{t+s} \\ s_{t+s-1} \end{bmatrix}, \tag{9}$$

where $\hat{A} = (I - bp)^{-1}(A + bm)$ and

$$f(l, k, s_{t-1}) = \left\{ c_t : \Psi A^k \hat{A} \begin{bmatrix} c_t \\ s_{t-1} \end{bmatrix} = -\Psi (I - A)^{-1} (I - A^k) b\bar{r} \right\}. \tag{10}$$

Here, $\Psi = \begin{bmatrix} I & -\Omega \end{bmatrix}$ where $\Omega : c_t = \Omega s_{t-1}$ represents the linear rational expectations solution of the unconstrained system as given, e.g., in Blanchard and Kahn (1980).

Finding the equilibrium values of (l, k) must be done numerically. The crucial advantage of the above representation over alternative methods such as Guerrieri and Iacoviello (2015) is that the simulation of anticipated trajectories (and matrix inversions at runtime) can be avoided when iterating over (l, k). This lends a reduction in computation time by a factor of roughly 1,500, which is necessary for our application. Ultimately, the resulting transition function is a nonlinear state-space representation.

3.2 Filtering and Estimation Method

Likelihood inference of models with an OBC requires a nonlinear Bayesian filter (e.g. An and Schorfheide, 2007; Herbst and Schorfheide, 2019). Given the high dimensionality of our model, the particle filter is not a feasible choice. As documented in Boehl and Strobel (2022), the *inversion filter* used in Guerrieri and Iacoviello (2017) and discussed in Cuba-Borda et al. (2019), for example, has a number of shortcomings that may render a correct likelihood inference difficult

when the filter is applied to medium-scale models.[4]

To bridge this gap, Boehl and Strobel (2022) introduce the Ensemble Kalman Filter (EnKF, Evensen, 1994) which can be understood as a hybrid of the particle filter and the Kalman filter. The EnKF is initialized by sampling an *ensemble* of particles from the initial distribution at $t = 0$. For each new observable at t, instead of re-sampling (particle filter), the EnKF applies statistical linearization to update the time-t state estimate, (which again is represented by the ensemble) to match each new observation vector. This allows us to efficiently approximate the distribution of states for large-scale nonlinear systems with only a few hundred particles instead of several million or billion, as with the particle filter, which is computationally advantageous.[5] For a more detailed discussion of the properties of the EnKF, see Boehl and Strobel (2022) and Katzfuss et al. (2016). To obtain the smoothed/historic shock innovations, we use a nonlinear path-adjustment smoother for high-dimensional nonlinear models, which is also proposed by Boehl and Strobel (2022).

We sample from the posterior distribution using the DIME MCMC sampler developed in Boehl (2022b). DIME a MCMC sampler and at the same time a gradient-free global multi-start optimizer. The sampler is shown to be robust for odd shaped, multimodal distributions and, due to its ensemble structure, trivially to parallelizable. For each estimation, we initialize an ensemble of 200 particles with the prior distribution and run 2500 iterations. Of these, we keep 500 to represent the posterior distribution. This representation hence entails a sample of $200 \times 500 = 100.000$ parameter vectors.

3.3 Data and Priors

For the quantitative analysis of the Great Recession and its aftermath, we use data spanning the period from 1964:I to 2019:IV in our benchmark sample. As documented by Boehl and Strobel (2022), the inclusion of the ELB period in the sample employed in the estimation matters for the model-implied interpretation of the Great Recession. In addition, we also consider samples that start in later years (1983:I and 1998:I) and therefore have a narrower focus on the events of the Great Recession.

To allow for a direct comparison of the marginal data densities, we estimate the RANK and the FRANK model on the same set of observables. These are real GDP growth, real consumption growth, real investment growth, labor hours, the log change of the GDP deflator, real wage growth,

[4]The filter is based on inverting the mapping between shocks and observables. For the medium-scale models considered here, this mapping is not unique, which can result in noisy likelihood estimates. Additionally, the proposed filter is not a Bayesian filter in a narrow sense and ignores uncertainty on the initial states and the observations.

[5]For all estimations and for the numerical analysis, we use an ensemble of 400 particles. This number is chosen to minimize sampling errors during likelihood inference. For the same reason we sample the initial distribution of states from quasi-random low-discrepancy series (e.g. Niederreiter, 1988). For our model, the evaluation of the likelihood for one parameter draw then would take about 2 seconds on a single CPU.

the Federal Funds Rate and the BAA spread. For this purpose, we augment the RANK model with an observation equation that links an exogenous AR(1) process directly to the observable spread. Importantly, this exogenous process stands apart from the other model equations such that it does not affect the behaviour of agents in the model.

The measurement equations that relate the model variables to our data series are

$$\text{Real GDP growth} = \overline{\gamma} + (y_t - y_{t-1} + z_t), \tag{11}$$

$$\text{Real consumption growth} = \overline{\gamma} + (c_t - c_{t-1} + z_t), \tag{12}$$

$$\text{Real investment growth} = \overline{\gamma} + (i_t - i_{t-1} + z_t), \tag{13}$$

$$\text{Real wage growth} = \overline{\gamma} + (w_t - w_{t-1} + z_t), \tag{14}$$

$$\text{Labor hours} = \bar{l} + l_t, \tag{15}$$

$$\text{Inflation} = \overline{\pi} + \pi_t, \tag{16}$$

$$\text{Federal Funds Rate} = (\frac{\overline{\pi}}{\beta\gamma^{-\sigma_c}} - 1) * 100 + r_t, \tag{17}$$

$$\text{BAA-spread} = \overline{spread} + spread_t. \tag{18}$$

where in the FRANK model, $spread_t$ is defined as $E_t[\widetilde{r}^k_{t+1} - r_t]$ and for RANK it follows an AR(1) process. The construction of the observables is mostly standard and delegated to Appendix A. Consistent with the detrending of nonstationary variables, the growth rate of technology, z_t in deviations from its steady state enters the measurement equations.

Notably, we set the empirical lower bound of the nominal interest rate within the model to 0.05% quarterly. Setting it exactly to zero would imply that the ELB never binds in our estimations, as the observed series for the FFR stays strictly above zero. Our choice maintains that the ELB is considered binding throughout the period from 2009:I to 2015:IV. For the observable Federal Funds Rate we cut off any value below 0.05. This ensures that any observable value is also in the domain of the model.[6]

We assume small measurement errors for all variables with a variance that is 0.01 times the variance of the respective series. Since the Federal Funds Rate is perfectly observable (though on a higher frequency) we divide the measurement error variance here again by 100. Hence, the observables are de facto matched perfectly.

In the calibration of some parameters and the choice of the priors for the estimation of the others we stick as closely as possible to the previous literature. For the parameters of RANK we rely on the choices of Smets and Wouters (2007). For the parameters associated with the extension of the

[6]The lower bound for the quarterly nominal rate is $\bar{r} = -100(\frac{\overline{\pi}}{\beta\gamma^{-\sigma_c}} - 1) + 0.05$, where $\overline{\pi}$ is gross inflation and the parameters γ and σ_c denote the steady state growth rate and the coefficient of relative risk aversion, respectively.

financial sector we use the priors employed by Del Negro et al. (2015). In the choice of our prior for $\overline{\gamma}$, we follow Kulish et al. (2017). Importantly, they opt for a tighter prior for this parameter than Smets and Wouters (2007). Arguably the economy deviated strongly and persistently from its steady state during the Great Recession. In order to dampen the data's pull of the parameter down to the sample mean, we prefer the tight prior as well.[7]

4 A decomposition of the Great Recession

In this section, we contrast the estimated RANK and FRANK models, and their empirical performance for the post-2008 period. We first give a brief discussion of the parameter estimates and then quantify the empirical fit of the two models using estimates of the marginal data densities. We then give an account of the historical shock decomposition over the most recent sample.

4.1 Parameter estimates

Posterior estimates for the structural parameters of the two models are presented for all samples in Tables B.2 and B.3 in Appendix B. Overall, the estimates are well within the range of values previously presented in the literature.

For our benchmark sample (1964:I-2019:IV), we find that the coefficient of relative risk aversion σ_c is slightly above unity in the RANK model. Similarly, Kulish et al. (2017), who also include the last decade in their estimation, find σ_c to be close to unity. A value of σ_c close to one mutes the effect of variations in labor hours on consumption via the Euler equation, which is introduced through the non-separabilities in preferences. The reduction of this channel prevents the strong drop in labor hours during the crisis to exert an excessive downward pull on consumption. In contrast, in the FRANK model, the estimate of this parameter of 1.78 is above the prior mean.

Our estimates also share some similarities with those of Del Negro et al. (2015), who also present estimates for both models. The parameters for habit formation, h, and investment adjustment costs, S'', imply that the FRANK model assigns a substantially lower importance to real rigidities that the RANK model does. Also in line with findings by Del Negro et al. (2015), the slopes of the price and wage Phillips curves are slightly flatter in FRANK than in RANK. With the Calvo parameters $\zeta_p = 0.904$ (RANK) and 0.927 (FRANK), the price Phillips curve in both models are far flatter than in the original estimates by Smets and Wouters (2007) (0.65). Del Negro et al. (2015) show that the finding of a flat Phillips curve is supported by the inclusion of the spread as an observable.[8] Furthermore, the estimated Taylor rule in RANK features a higher interest rate

[7] For wider priors we confirm unrealistically low estimates of the trend growth rate.

[8] More specifically, Del Negro et al. (2015) argue that the deep recession in conjunction with the mild decline in inflation can be rationalized either by counteracting supply shocks or a flat Phillips curve. Including the spread as observable puts more weight on shocks that raise the spread and which happen to have demand shocks properties,

	USA			*Euro area*
	1964-2019	1983-2019	1998-2019	1998-2019
RANK	-1084.15	-524.80	-331.24	176.15
FRANK	-1177.89	-552.09	-354.08	138.55

Table 1: Comparison of Marginal Data Densities

smoothing parameter ρ and a stronger feedback to movements in inflation ϕ_π than in the FRANK model.

In line with the events of the financial crisis, those shocks that have been associated with financial factors – the risk premium shock, the MEI shock, and the financial shock - all feature a high persistence in both models.

4.2 Marginal data densities

As discussed in Section 3.3, we augment the RANK model with an extra equation in which an exogenous spread is linked to the observed spread in order to estimate both models on the same set of observables. This allows us to directly compare the two models using marginal data densities (MDD). The marginal data density, sometimes also referred to as the marginal likelihood, or the model evidence, is a central measure for the empirical fit of the model and states the probability of the data given the model and its priors.

Table 1 displays the MDD for the two models over the different samples as well as for the euro area. As it turns out, the introduction of financial frictions à la BGG worsens the empirical performance of the estimated model. The finding of a lower fit is robust to the length of the employed sample.[9] This is startling at first, since the Global Financial Crisis and the Great Recession were main motivators for modeling the linkages between the financial sector and the macroeconomy. Indeed, the introduction of financial friction allows for a model-consistent role of financial spreads for business cycle dynamics. As data on spreads are available earlier on than national accounts data, and as they are published at a higher frequency, this provides a substantial advantage for nowcasts and short-term forecasts in a financial crisis.[10] Nonetheless, as we discuss below, this does not imply that the incorporation of financial frictions delivers a better ex-post explanation of the observed macroeconomic series.

The model fit in terms of the MDD is closely linked to the historic decomposition as implied by the estimated model. To see this, note that, mathematically speaking, the MDD is the integral

supporting the explanation of the missing disinflation via a flat Phillips curve.

[9] Additionally, the result is also robust to an alternative specification of the observables in which we group durable consumption into the observed investment series, as in Justiniano et al. (2011).

[10] The better forecast performance of the model with financial friction is discussed in Del Negro and Schorfheide (2013); Del Negro et al. (2015); Cai et al. (2019).

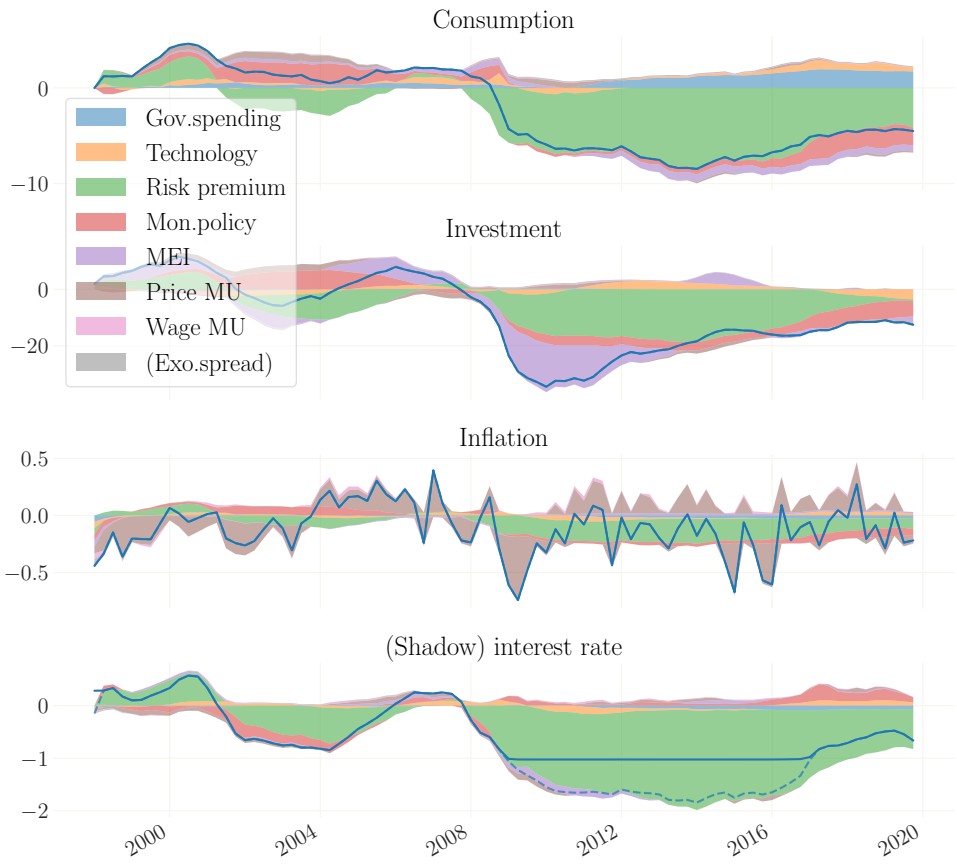

Figure 1: Historical shock decomposition of the Great Recession using the RANK Model estimated on the full sample from 1964–2019. Consumption and Investment: percentage deviations from their steady state growth path. Inflation and (shadow) interest rate: percentage point deviations from steady state. *Note:* Means over 250 simulations drawn from the posterior. The contribution of each shock is normalized as in Boehl and Strobel (2022).

over the prior distribution, i.e. the result of marginalizing over the parameter space. Thus, it is closely tied to those factors that also determine the likelihood. These comprise the uncertainty about initial states (i.e., the states prior to the first observation), potential measurement errors, the prior distribution, and the likelihood of the individual exogenous innovations. The initial states of both models are set in the same fashion using the stationary distribution. We also assume very small measurement errors and the priors are, apart from the additional variable ζ_{spb}, equal. Hence, the magnitude and distribution of exogenous innovations must be the main drivers of the differences documented in Table 1. In this regard, a model that attributes the economic dynamics of the observables to one main shock clearly has a larger MDD than a model in which several shocks must counteract each other in order to explain the observed time series.

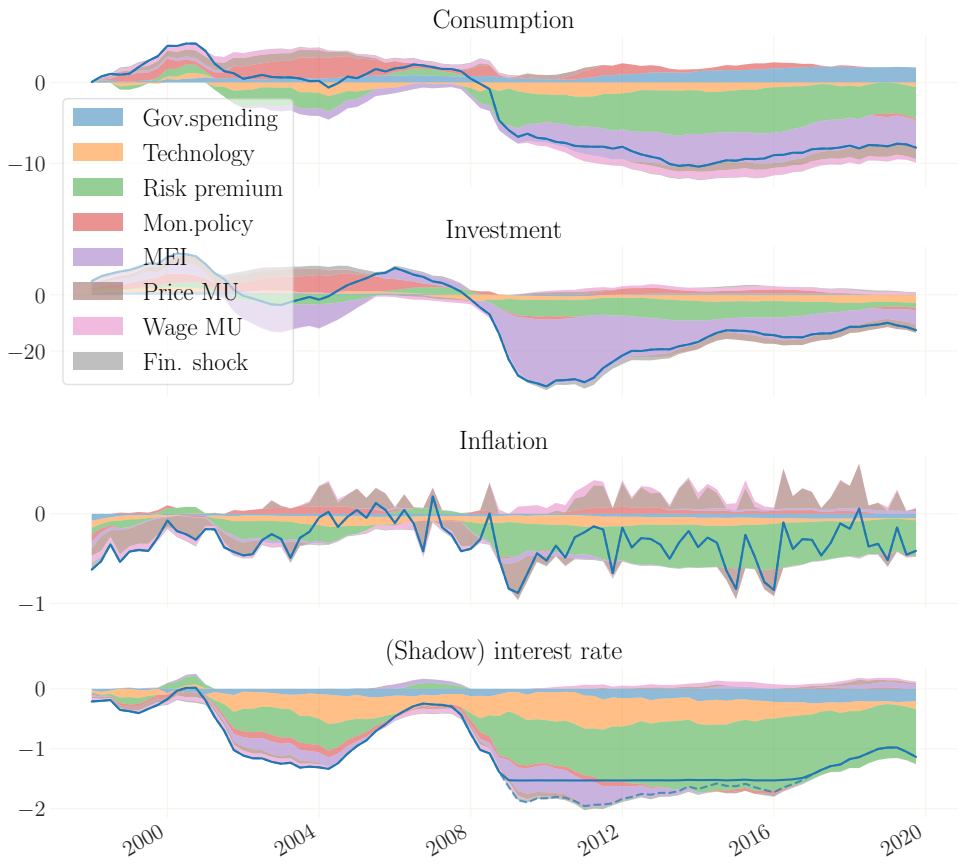

Figure 2: Historical shock decomposition of the Great Recession using the FRANK Model estimated on the full sample from 1964–2019. Consumption and Investment: percentage deviations from their steady state growth path. Inflation and (shadow) interest rate: percentage point deviations from steady state. *Note:* Means over 250 simulations drawn from the posterior. The contribution of each shock is normalized as in Boehl and Strobel (2022).

4.3 Historic shock decompositions

To explain the relatively poor performance of FRANK in terms of model fit documented in the previous section, we show historic shock decompositions of the economic dynamics since 1998 for both models. These are presented in Figures 1 and 2. We focus on the short sample because it allows us to zoom in on the post-2008 episode, which is at the core of our investigation. The results presented here, however, hold for the post-2008 episode regardless of the sample choice.

Historic shock decompositions of nonlinear models generally bear the problem that the ordering of shocks matters. Suggestions to circumvent this problem are based on the idea of nonlinear impulse response functions (e.g. Koop et al. (1996) and Lanne and Nyberg (2016)). These methods are based on sampling from the filtered shocks and are computationally rather expensive. Instead, and interesting as an independent contribution of its own, we propose a novel method to conduct historic decompositions for linearized economic models with occasionally binding constraints. Our method is able to precisely distinguish the linear and the nonlinear impact of each shock, thereby

remaining independent of any ordering effects. The quantitative nonlinear effect of a shock is calculated by its current and expected impact on the *constrained* variable. Boehl and Strobel (2022) provides details.

In the context of the RANK model, risk premiums shocks ϵ_t^μ are the most prominent driver of the joint dynamics of key variables following the financial crisis. Figure 1 illustrates the dominant role of this shock for macroeconomic dynamics following the Great Recession. From 2009 on, persistently elevated risk premiums account for almost the entire drop of aggregate consumption, weigh on aggregate investment and inflation, and are thus responsible for the long duration of the ELB spell for the nominal interest rate.[11]

However, high risk premiums cannot fully account for the sharp drop in investment during the Great Recession. While recessionary risk premium shocks do trigger a simultaneous downturn of consumption and investment, they fail to match the drop differential of these components, creating the need for an extra driver to make up for the missing decline in investment. In the case at hand, the initial decline in investment is triggered by recessionary MEI shocks, ϵ_t^i, which at the trough account for roughly half of the collapse in investment.

Similarly, the decline in inflation during the Great Recession can only partly be attributed to the increase in risk premiums. The estimated flat Phillips Curve prevents the decline in real activity from generating substantial deflation. It requires price markup shocks, ϵ_t^p, to account for the high-frequency movements of inflation in the sample and account for the dip in inflation during the Great Recession. The fact that inflation only decreased modestly triggered a debate on the missing disinflation puzzle. Christiano et al. (2015) attribute some inflationary pressure to a persistent decline in productivity relative to its pre-recession trend. In contrast, in our estimation, which abstracts from a separate TFP-specific trend, the technology process, z_t, is consistently measured to be positive. In addition, Christiano et al. (2015) as well as Gilchrist et al. (2017) ascribe the missing inflation to higher refinancing costs of firms. We cannot confirm within the RANK model that MEI shocks, which increase the firms' cost of investments, raise inflation. Instead, in our analysis and similarly to Del Negro et al. (2015), the estimate of a flat Phillips Curve is responsible for the lack of a steep decline in inflation.

The long duration of the ELB is largely interpreted by our estimation as an endogenous response of the central bank to the deterioration of fundamentals via the Taylor rule, rather than to

[11] Christiano et al. (2015) label this shock *consumption wedge*, contrasting it with the *financial wedge* that is captured by the MEI shocks in our analysis. Smets and Wouters (2007) compare the effects of the shock to those of disturbances to net worth of entrepreneurs in a model with financial frictions as in Bernanke et al. (1999). Fisher (2015) offers a structural interpretation of the risk premium shock as a shock to the demand for safe and liquid assets. Each of these interpretations share the notion that the risk premium shock is a short cut for capturing some financial disturbances, which makes its prominent role in the Great Recession plausible.

an active lower-for-longer policy. [12]

The reliance on disparate exogenous drivers for the explanation of the dynamics of key variables during the Great Recession is a shortcoming of the RANK model. Nonetheless, Figure 2 shows that in FRANK, this problem is exacerbated. Notably, the dynamics of consumption and investment are driven by two disparate sources of shocks. This represents a severe drawback for the FRANK model's appeal, as it moves farther away from providing a unifying account of macroeconomic dynamics in the Great Recession than RANK. While the financial sector itself acts as an attenuator for output and investment dynamics, the higher persistence of MEI shocks in FRANK supports a more pronounced decline in aggregate demand, thereby creating deflationary pressure. As with RANK, this pressure is too weak to cause the dip in inflation during the Great Recession. Again, the inability of the model to account for the inflation dynamics is associated with a flat Phillips Curve and variations in inflation are largely attributed to exogenous fluctuations in the price markup. We see the lack of a joint propagation mechanism as the main driver for the rather poor empirical performance of FRANK relative to RANK. In Section 5 we will study the underlying mechanisms in detail.

5 The Role of Financial Frictions

The financial crisis and the subsequent Great Recession triggered an active literature on the role of financial frictions for macroeeconomic dynamics. In this section, we focus on the discussion of the Great Recession through the lens of the FRANK model, which adds financial frictions a la Bernanke et al. (1999) to the canonical Smets and Wouters (2007) model. As documented in the previous section, this extension of the model does not improve the performance of the model in explaining the Great Recession. This is due to the fact that the model-implied procyclicality of the leverage in this episode is at odds with the observed countercyclical interest rate spreads. In addition, the decline in the leverage attenuates the effects of shocks to the risk premium and MEI shocks on investment. Thus, the model with financial frictions requires larger shocks to explain the collapse of investment in the Great Recession than the RANK model. We further show that the *risk shock* à la Christiano et al. (2014), i.e. a disturbance on the financial friction, does not increase the explanatory power of the model.

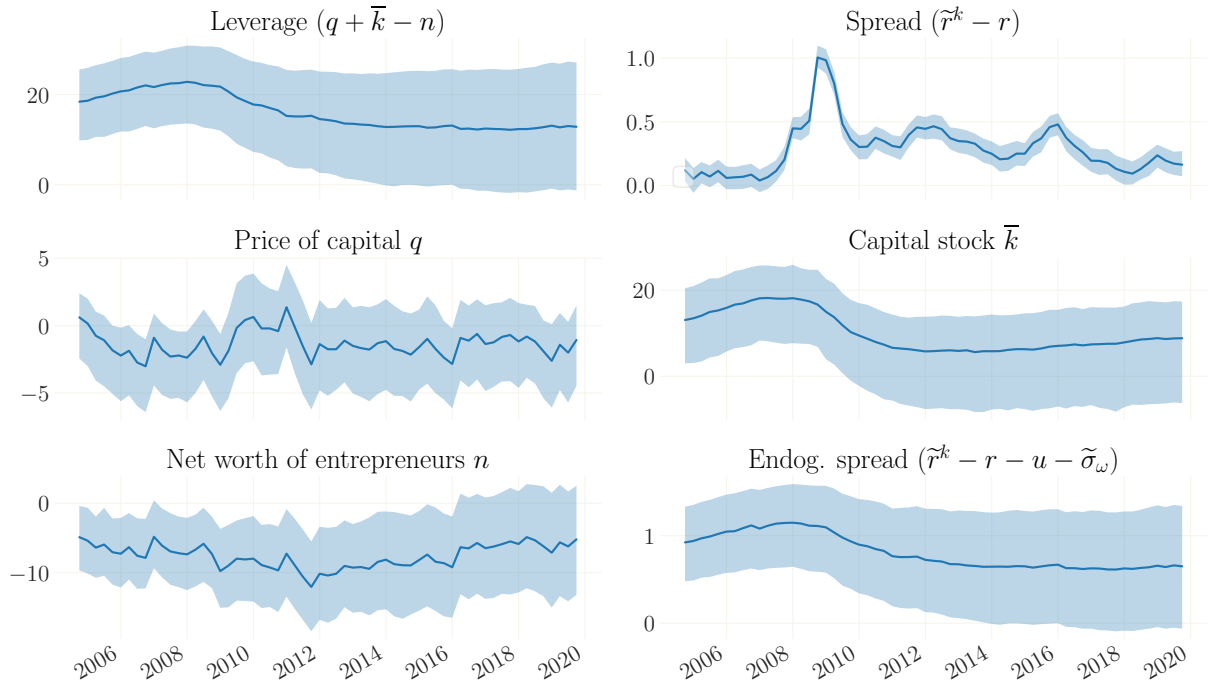

Figure 3: Model implied dynamics for spread, leverage and its ingredients in FRANK *Note:* Means over 250 simulations drawn from the posterior distribution; the shaded area depicts 95% credible sets.

5.1 Empirical fit: obseved spread and model-implied leverage

The difference between RANK and FRANK is that in the financial frictions model, the required return on capital is linked to the leverage of entrepreneurs (see section 2.2). In addition, the leverage is subject to financial shocks. By construction, a higher leverage increases the default probability of entrepreneurs in the model: to compensate for the increased risk of default, investors charge a higher spread when the leverage is high. This condition is captured by Equation 4, which is repeated here for convenience:

$$E_t[\widetilde{r}^k_{t+1} - r_t] = u_t + \zeta_{sp,b}(q_t + \overline{k}_t - n_t) + \widetilde{\sigma}_{\omega,t}.$$

This endogenous relation between the leverage ratio and the spread – captured by $\zeta_{sp,b}(q_t + \overline{k}_t - n_t)$ – is at odds with the implications of the estimated model. Figure 3 shows that the model-implied leverage ratio of entrepreneurs gradually increases before 2009, and markedly declines afterwards.

[12]The mean expected durations vary between four and ten quarters throughout the ELB years. Though we do not target, nor use, any prior information on the actual expectations of market participants on the duration of the ELB, they are broadly comparable to the average expected durations reported by the Blue Chip Financial Forecast and the New York Fed's Survey of Primary Dealers. On average, our estimates of the expected durations are in between those of Gust et al. (2017) and Kulish et al. (2017). For a more detailed comparison of the results for different methods for estimating ELB durations, see Boehl and Strobel (2022).

At same time, the spread, which is directly linked to the observed BAA-spread, remains elevated after its sharp spike at the height of the recession.

The decline in the leverage ratio generated by the model broadly aligns with the observed de-leveraging of publicly listed firms in the United States in the years after 2008, particularly of financial firms (see Appendix D). Adrian and Shin (2014) explain this behavior of financial firms with their motive to shed risk and to effectively stabilize their probability of default by maintaining a stable Value-at-Risk over their equity.[13] This first-pass comparison between the endogenously generated dynamics of the leverage ratio in the estimated FRANK model and an empirical measure of the aggregate leverage of US firms lends credence to our results. However, any closer comparison should be taken with a grain of salt as several plausible candidates for an empirical measure of the aggregate leverage of US firms exist, which can display quite different dynamics. We document this in Appendix D.

In the estimated model, this deleveraging can be traced back to the substantial decline in the capital stock, which is depressed by the collapse of investment in the Great Recession. At the same time, the model generates a price of capital that is somewhat elevated after 2010 while suggesting that the net worth of entrepreneurs remains largely flat. This divergence between the spread and its endogenous driver (the leverage ratio) must be compensated by the exogenous risk premium shocks u_t and the financial shock $\widetilde{\sigma}_{\omega,t}$. Hence, the one additional feature in FRANK that aims at endogenizing the behavior of the spread fails to explain its dynamics after the Great Recession. The exogenous shocks necessary to repair this failure and to reconcile the dynamics of the spread with the dynamics of the observed macroeconomic series worsens the empirical fit of the model.

5.2 The role of the financial sector for the transmission of shocks

The inclusion of the financial sector also alters the transmission of shocks in important ways. The posterior distribution of the parameter estimates for FRANK on the full sample (see Table B.3) shows that the estimated persistence parameters of risk premium shocks as well as of MEI shocks are substantially higher in FRANK than in RANK. The effects of these shocks are therefore more pronounced and persistent in FRANK than in RANK.[14] Figure 4 illustrates this for the dynamic response of key variables to a positive risk premium shock.

At the same time, however, the risk premium shock in the estimated FRANK model performs worse than the RANK model in generating the relative drop-differential of investment and consumption observed in the Great Recession. On the one hand this is due to the mean estimate of

[13] More specifically, Adrian and Shin (2014) document in Fig. 5 of their paper that large commercial and investment banks substantially delevered in the years after the Bear Stearns crisis in March 2008.

[14] The higher persistence of the effect risk premium shocks in the FRANK model than in the RANK model is in line with previous findings by Cai et al. (2019).

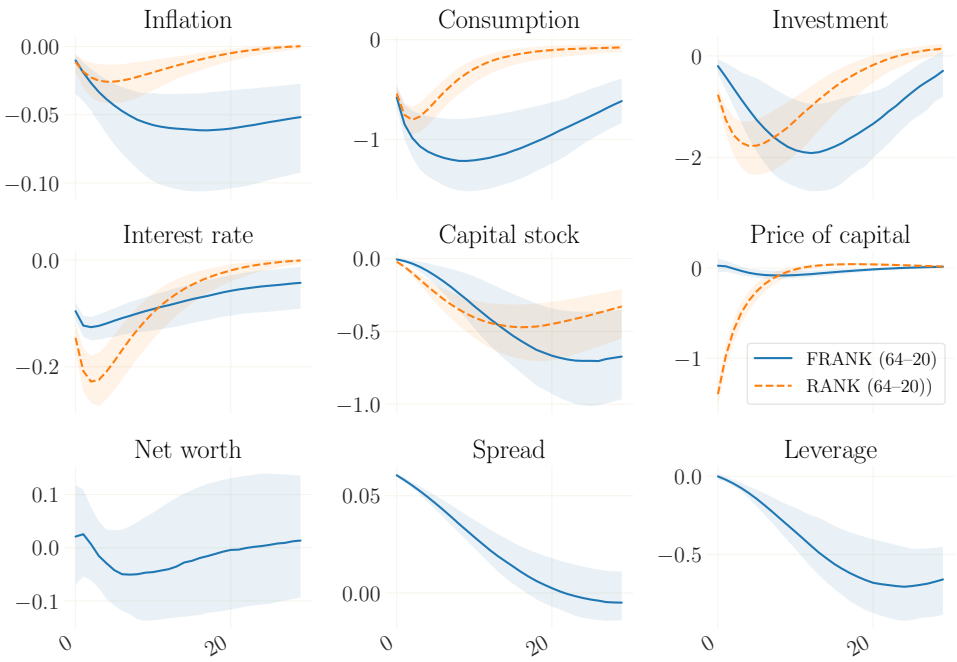

Figure 4: Impulse responses to risk premium shock of one standard deviation. *Note:* Medians over 250 simulations drawn from the posterior. The shaded area depicts the 90% credible set. For each model the shock size equals the posterior mean standard deviation of the shock.

the coefficient of relative risk aversion, which is quite high ($\sigma_c = 1.782$). This activates the non-separabilities in the utility function, such that the decline in labor hours in the Great Recession generates excessive downward pressure on aggregate consumption.

Secondly, the financial sector acts as an attenuator of the effects of risk premium shocks on investment. As Figure 4 shows, the risk premium shock increases the spread charged by creditors. However, at the same time it reduces the leverage of entrepreneurs. In response to the shock, the drop in investment lowers the capital stock, but decline in the price of capital and entrepreneurial net worth is rather modest. The subsequent reduction in leverage compresses the spread that investors demand from entrepreneurs. Hence, the response of the required return on investment is reduced relative to RANK, which in turn lowers the appeal of risk premium shocks for explaining the Great Recession in the FRANK model.

As can be seen in Figure 5, the effects of MEI shocks are altered in the FRANK model as well. While the decline in consumption in response to a recessionary MEI shock constitutes an improvement relative to the estimated RANK model, in which MEI shocks induce a negative co-movement of consumption and investment, the financial sector again acts as an attenuator for investment. More importantly, MEI shocks are supply shocks on the financial markets, which increase the price of capital while reducing investment and raising entrepreneurial net worth. As a result, this lowers the entrepreneurial leverage and therefore the credit spread. Hence, the shock

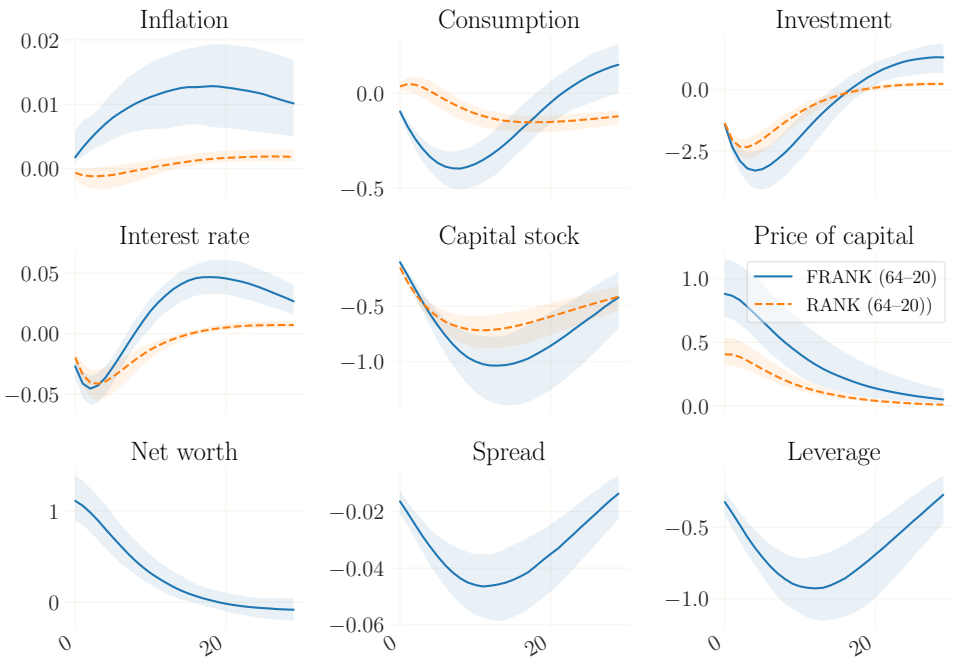

Figure 5: Impulse responses to a MEI shock of one standard deviation. Financial variables for RANK are calculated *as if*, i.e. excluding taking their general equilibrium effects into account.
Note: Medians over 250 simulations drawn from the posterior. The shaded area depicts the 90% credible set. For each model the shock size equals the posterior mean standard deviation of the shock.

induces a positive co-movement of investment and the financial spread, which is at odd with the data. This presents a severe drawback of MEI shocks in the FRANK model and rules them out as a candidate for a main driver of joint dynamics of macroeconomic and financial variables in the Great Recession.

5.3 Can risk shocks explain the Great Recession?

One advantage of modeling the financial sector is the ability to incorporate financial shocks and study their effect on the real economy. At first glance, this appears particularly appealing when analyzing the Great Recession. The financial shock in the FRANK model is the risk shock, which was developed by Christiano et al. (2014). The risk shock is an exogenous process driving changes in the volatility of cross-sectional idiosyncratic uncertainty of entrepreneurs.

As Figure 6 shows, an increase in entrepreneurial risk raises the credit spread and makes external funding less affordable for entrepreneurs. Aggregate investment and the price of capital therefore both drop, together with entrepreneurial net worth. In contrast to the MEI shock, which drives Tobin's Q and investment in opposite directions, the risk shock is therefore a demand shock in the market for investment goods. The drop in investment demand lowers output and hence labor hours. Given, the non-separabilities in the preferences of households, the decline in labor reduces

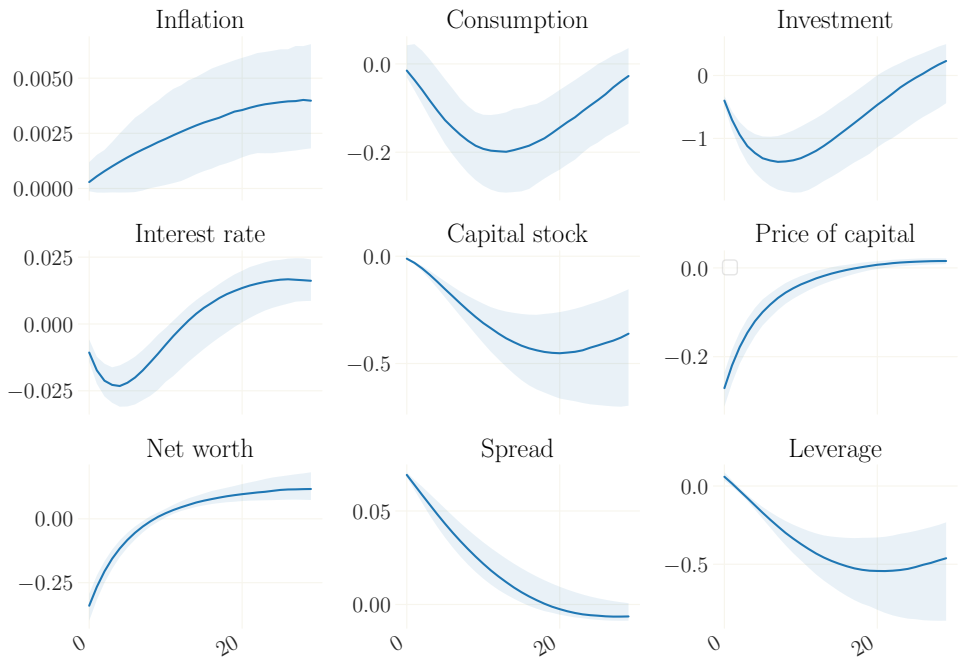

Figure 6: Impulse responses to risk shock (i.e. the financial shock) of one standard deviation in FRANK.
Note: Medians over 250 simulations drawn from the posterior. The shaded area depicts the 90% credible set. The shock size equals the posterior mean standard deviation of the shock.

consumption. With regard to the post-2008 course of inflation, a feature of the risk shock is that, by raising the costs of capital, it increases marginal cost and thus creates inflationary pressure. However, whereas the risk shock in principle speaks to the missing deflation puzzle, the outright increase in inflation is at odds with observed price dynamics after the recession. As an additional drawback, the higher inflation rate puts upward pressure on the nominal interest rate via the Taylor rule such that the decline in the policy rate after the shock is short-lived. The risk shock therefore cannot explain the drop in the nominal interest towards the effective lower bound.[15]

Accordingly, the estimated standard deviation of financial shocks is rather small and the effect of the shock on macroeconomic variables is weak compared, for example, to the effect of a one standard deviation risk premium shock. The historic shock decomposition (see Figure 2 in Appendix B) confirms that the role of the financial shock for macroeconomic dynamics is not very prominent. Allowing the risk shock to affect the real economy therefore does not improve upon the explanation of macroeconomic dynamics as given by RANK.

Our result confirms a similar finding by Christiano et al. (2014). The authors document that

[15]In an estimation of the model on a sample that starts in 1983 and therefore has a narrower focus on the last few decades, the risk shock in the spirit of Christiano et al. (2014) is prone to inducing a negative co-movement of investment and consumption. This issue is shared by other financial shocks in the literature (see, e.g., the investment and the credit shock in Carlstrom et al. (2017) or the wealth shock in Carlstrom and Fuerst (1997).

the importance of the risk shock hinges on the inclusion of more financial variables in the set of observables. For the purpose of this paper, we abstain from walking that path. Using additional variables in the estimation raises the risk that the likelihood is dominated by non-macroeconomic observables, making a close comparison with the RANK model difficult. Additionally, as we document in Appendix D, it is not straightforward to select the adequate observables for financial quantities. Several plausible candidates exist that imply very different dynamics for the aggregate US leverage ratio. Some are only available for a few decades, restricting the estimation sample. Thus, we keep the set of observables unaltered and focus on the explanatory power of the BGG-type of friction for macroeconomic dynamics.

6 Post-2008 dynamics in the euro area

The unfolding of the financial crisis in the euro area as well as the conduct of monetary policy differed in many aspects from the developments in the United States. Notably, the crisis in the euro area was extended by the sovereign debt crisis and capital flight from southern Europe. In this setting – and in step with the ECBs longer-term refinancing operations and asset purchase programmes – euro area banks' holdings of excess reserves at the ECB skyrocketed. The overnight rate in the interbank market, which prior to the crisis was closely aligned with the ECB's rate on marginal refinancing operations now started tracking the rate of the deposit facility (DFR), which the ECB eventually steered into negative territory.

To accommodate the negative interest rate, while maintaining the concept of an effective lower bound, we propose an adjustment to the RANK and the FRANK model. Importantly, we assume that agents in the euro area did not expect the rate on reserves to dive into negative territory. This can be justified by the high costs associated with negative interest as well as with the reluctance of central banks to set negative interest rates even at the height of the financial crisis. Such a perceived lower bound (PLB), although arguably only an intellectual constraint, can have a large impact on economic dynamics. Hence, we assume that while in positive territory, the ECB's rate on reserves, r_t^+ follows the policy rule for the notional rate, r_t^n spelled out in Equation 3. The interest rate on reserves (IOR), r_t, thus follows

$$r_t = \max\{0, r_t^n\} + v_t^{nir}, \tag{19}$$

where we put the stochastic negative interest rate process v_t^{nir} – which follows an AR(1) process – outside the max operator to allow for policy innovations that drive the IOR rate into negative territory, while having agents expect a classic lower bound on the nominal rate ex-ante.

This design of the lower bound has consequences for the observation equations used in the estimation of the model. Instead of using the IOR observable (the EONIA) directly, it is further divided into IOR+ = $\max\{IOR, 0\}$ and NIR = $\min\{IOR, 0\}$. This helps to identify the impact of the

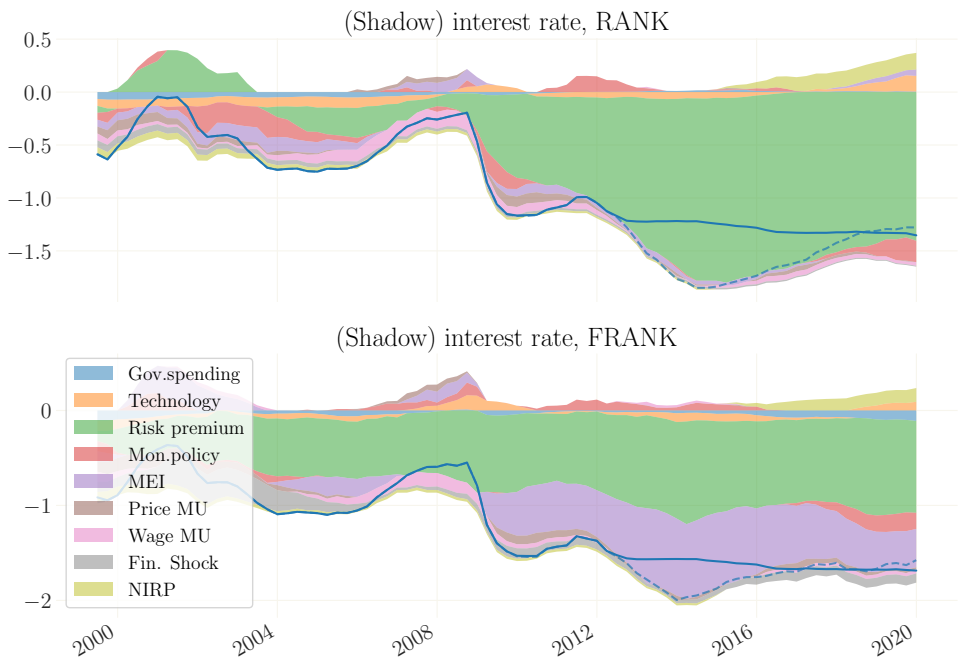

Figure 7: Historical shock decomposition of interest rates in the euro area using the RANK and FRANK Model. Variables in percentage point deviations from their steady state growth path. *Note:* Means over 250 simulations drawn from the posterior. The contribution of each shock is normalized as in Boehl and Strobel (2022).

PLB and to quantify the effects of the NIR policy. Additionally, the set of observables includes the real per capita growth rates of euro area GDP, consumption, and investment, real wage growth, a measure of labor hours, the GDP deflator, and the BAA yield as a measure of the credit spread. In addition to the disturbances also used in the models for the US, we add the negative interest rate policy shock. For our estimation, we consider a sample from 1998:I-2019:IV. Further details are delegated to Appendix A.

As it turns out, the poor empirical performance of the financial accelerator framework extends to euro area data as well. The marginal data density (MDD) for the FRANK model (138.6) lies well below the MDD for the RANK model (176.2). Figure 7 shows that, as in the case of the US, the risk premium shock is the main driver of the recessionary dynamics in the RANK model, pushing the policy rate towards zero. Also as in the US, Figure 7 shows that the introduction of financial frictions in the FRANK model, reduces the importance of the risk premium shock and cocomitantly the model's ability to offer a common cause for the dynamics of macroeconomic variables in the crisis. In the FRANK model, both MEI and risk premium shocks are major drivers of the recession. The role of financial shocks remains minor. Overall, this analysis underlines that in the Euro area the FRANK model as well has difficulties in reconciling macroeconomic and financial dynamics.

7 Conclusion

This paper presents a step towards the evaluation of the empirical performance of financial frictions in medium-scale models with a focus on the Great Recession in the US. We document that although the empirical performance of the RANK model calls for improvements, the extended model that includes financial frictions as in Bernanke et al. (1999) has a lower empirical fit. This can be traced back to the divergent dynamics of the leverage ratio and the credit spread after the recession. Additional shocks are needed to reconcile the phenomenon of continually elevated spreads with the marked deleveraging in the model. The finding that the inclusion of BGG-type frictions does not improve upon the empirical fit of the medium-scale model is robust to shorter US samples and extends to the analysis of the financial crisis in the euro area as well.

Our evaluation of financial frictions centers on the prominent framework of BGG. Its difficulties to provide a good ex-post account of the Great Recession does not dismiss its use for other purposes such as, e.g., forecasting. Nor does it dismiss the importance of financial frictions per se: many alternative specifications of financial frictions exist that may help to fit macroecnomic models to post-2008 data. In particular, our findings point towards frictions in household financing to be promising candidates. Decomposing the US and euro area dynamics after the Great Recession into the contribution of its causal drivers using the RANK model, we find that post-2008 dynamics are dominated by elevated risk premiums on household borrowing rates, in line with the importance of increased mortgage rates in the financial crisis. Going forward, it is a fruitful endeavor to use more refined models that zoom in on the drivers of elevated risk premiums.

References

Adrian, Tobias and Hyun Song Shin, "Procyclical Leverage and Value-at-Risk," *Review of Financial Studies*, 2014, *27* (2), 373–403.

An, Sungbae and Frank Schorfheide, "Bayesian analysis of DSGE models," *Econometric reviews*, 2007, *26* (2-4), 113–172.

Bernanke, Ben S, Mark Gertler, and Simon Gilchrist, "The financial accelerator in a quantitative business cycle framework," *Handbook of Macroeconomics*, 1999, *1*, 1341–1393.

Blanchard, Olivier Jean and Charles M Kahn, "The solution of linear difference models under rational expectations," *Econometrica: Journal of the Econometric Society*, 1980, pp. 1305–1311.

Boehl, Gregor, "Efficient solution and computation of models with occasionally binding constraints," *Journal of Economic Dynamics and Control*, 2022, *143*, 104523.

_ , "Ensemble MCMC Sampling for Robust Bayesian Inference," *Available at SSRN 4250395*, 2022.

_ **and Felix Strobel**, "Estimation of DSGE Models with the Effective Lower Bound," Discussion Paper Series CRC TR 224, University of Bonn and University of Mannheim, Germany 2022.

_ **, Gavin Goy, and Felix Strobel**, "A structural investigation of quantitative easing," *Review of Economics and Statistics*, forthcoming.

Brzoza-Brzezina, Michal and Marcin Kolasa, "Bayesian Evaluation of DSGE Models with Financial Frictions," *Journal of Money, Credit and Banking*, 2013, *45* (8), 1451–1476.

Cai, Michael, Marco Del Negro, Marc P. Giannoni, Abhi Gupta, Pearl Li, and Erica Moszkowski, "DSGE forecasts of the lost recovery," *International Journal of Forecasting*, 2019, *35* (4), 1770–1789.

Calvo, Guillermo A, "Staggered prices in a utility-maximizing framework," *Journal of Monetary Economics*, 1983, *12* (3), 383–398.

Carlstrom, Charles T and Timothy S Fuerst, "Agency Costs, Net Worth, and Business Fluctuations: A Computable General Equilibrium Analysis," *American Economic Review*, December 1997, *87* (5), 893–910.

Carlstrom, Charles T., Timothy S. Fuerst, and Matthias Paustian, "Optimal Contracts, Aggregate Risk, and the Financial Accelerator," *American Economic Journal: Macroeconomics*, January 2016, *8* (1), 119–47.

_ **,** _ **, and** _ , "Targeting Long Rates in a Model with Segmented Markets," *American Economic Journal: Macroeconomics*, January 2017, *9* (1), 205–42.

Christensen, Ian and Ali Dib, "The Financial Accelerator in an Estimated New Keynesian Model," *Review of Economic Dynamics*, January 2008, *11* (1), 155–178.

Christiano, Lawrence J., Martin S. Eichenbaum, and Mathias Trabandt, "Understanding the Great Recession," *American Economic Journal: Macroeconomics*, January 2015, *7* (1), 110–67.

_ **, Roberto Motto, and Massimo Rostagno**, "Risk Shocks," *American Economic Review*, January 2014, *104* (1), 27–65.

Cuba-Borda, Pablo, Luca Guerrieri, Matteo Iacoviello, and Molin Zhong, "Likelihood evaluation of models with occasionally binding constraints," *Journal of Applied Econometrics*, 2019, *34* (7), 1073–1085.

Darracq Pariès, Matthieu, Christoffer Kok Sørensen, and Diego Rodriguez-Palenzuela, "Macroeconomic Propagation under Different Regulatory Regimes: Evidence from an Estimated DSGE Model for the Euro Area," *International Journal of Central Banking*, December 2011, *7* (4), 49–113.

Del Negro, Marco and Frank Schorfheide, "DSGE Model-Based Forecasting," in G. Elliott, C. Granger, and A. Timmermann, eds., *Handbook of Economic Forecasting*, Vol. 2 of Handbook of Economic Forecasting, Elsevier, 2013, chapter 0, pp. 57–140.

_ **, Marc P Giannoni, and Frank Schorfheide**, "Inflation in the Great Recession and New Key-

nesian models," *American Economic Journal: Macroeconomics*, 2015, *7* (1), 168–96.

Evensen, Geir, "Sequential data assimilation with a nonlinear quasi-geostrophic model using Monte Carlo methods to forecast error statistics," *Journal of Geophysical Research: Oceans*, 1994, *99* (C5), 10143–10162.

_ , *Data assimilation: the ensemble Kalman filter*, Vol. 2, Springer, 2009.

Fisher, Jonas D.M., "On the Structural Interpretation of the Smets–Wouters "Risk Premium" Shock," *Journal of Money, Credit and Banking*, 2015, *47* (2-3), 511–516.

Gertler, Mark and Peter Karadi, "A model of unconventional monetary policy," *Journal of Monetary Economics*, 2011, *58*, 17–34.

Gilchrist, Simon and Benoit Mojon, "Credit Risk in the Euro Area," *The Economic Journal*, 2018, *128* (608), 118–158.

_ **, Raphael Schoenle, Jae Sim, and Egon Zakrajšek**, "Inflation Dynamics during the Financial Crisis," *American Economic Review*, March 2017, *107* (3), 785–823.

Goodman, Jonathan and Jonathan Weare, "Ensemble samplers with affine invariance," *Communications in applied mathematics and computational science*, 2010, *5* (1), 65–80.

Graeve, Ferre De, "The external finance premium and the macroeconomy: US post-WWII evidence," *Journal of Economic Dynamics and Control*, 2008, *32* (11), 3415–3440.

Guerrieri, Luca and Matteo Iacoviello, "OccBin: A toolkit for solving dynamic models with occasionally binding constraints easily," *Journal of Monetary Economics*, 2015, *70*, 22–38.

_ **and** _ , "Collateral constraints and macroeconomic asymmetries," *Journal of Monetary Economics*, 2017, *90* (C), 28–49.

Guerrieri, Veronica and Guido Lorenzoni, "Credit Crises, Precautionary Savings, and the Liquidity Trap*," *The Quarterly Journal of Economics*, 03 2017, *132* (3), 1427–1467.

Gust, Christopher, Edward Herbst, David López-Salido, and Matthew E Smith, "The empirical implications of the interest-rate lower bound," *American Economic Review*, 2017, *107* (7), 1971–2006.

Herbst, Edward and Frank Schorfheide, "Tempered particle filtering," *Journal of Econometrics*, 2019, *210* (1), 26–44.

Justiniano, Alejandro, Giorgio Primiceri, and Andrea Tambalotti, "Investment Shocks and the Relative Price of Investment," *Review of Economic Dynamics*, January 2011, *14* (1), 101–121.

Katzfuss, Matthias, Jonathan R Stroud, and Christopher K Wikle, "Understanding the ensemble Kalman filter," *The American Statistician*, 2016, *70* (4), 350–357.

Kehoe, Patrick J, Pierlauro Lopez, Virgiliu Midrigan, and Elena Pastorino, "Credit Frictions in the Great Recession," Working Paper 28201, National Bureau of Economic Research December 2020.

Kimball, Miles S., "The Quantitative Analytics of the Basic Neomonetarist Model," NBER Work-

ing Papers 5046, National Bureau of Economic Research, Inc February 1995.

Kiyotaki, Nobuhiro and John Moore, "Credit Cycles," *Journal of Political Economy*, April 1997, *105* (2), 211–248.

Koop, Gary, M Hashem Pesaran, and Simon M Potter, "Impulse response analysis in nonlinear multivariate models," *Journal of econometrics*, 1996, *74* (1), 119–147.

Kulish, Mariano, James Morley, and Tim Robinson, "Estimating DSGE models with zero interest rate policy," *Journal of Monetary Economics*, 2017, *88*, 35 – 49.

Lanne, Markku and Henri Nyberg, "Generalized Forecast Error Variance Decomposition for Linear and Nonlinear Multivariate Models," *Oxford Bulletin of Economics and Statistics*, August 2016, *78* (4), 595–603.

Mian, Atif and Amir Sufi, "What Explains the 2007–2009 Drop in Employment?," *Econometrica*, 2014, *82* (6), 2197–2223.

_ and _, *House of Debt* number 9780226271651. In 'University of Chicago Press Economics Books.', University of Chicago Press, 2015.

Niederreiter, Harald, "Low-discrepancy and low-dispersion sequences," *Journal of number theory*, 1988, *30* (1), 51–70.

Rannenberg, Ansgar, "Bank Leverage Cycles and the External Finance Premium," *Journal of Money, Credit and Banking*, 2016, *48* (8), 1569–1612.

Smets, Frank and Raf Wouters, "Shocks and frictions in US business cycles: A Bayesian DSGE approach," *American Economic Review*, 2007, *97* (3), 586–606.

Verona, F., M. M. F. Martins, and I. Drumond, "(Un)anticipated Monetary Policy in a DSGE Model with a Shadow Banking System," *International Journal of Central Banking*, September 2013, *9* (3), 78–124.

Villa, Stefania, "FINANCIAL FRICTIONS IN THE EURO AREA AND THE UNITED STATES: A BAYESIAN ASSESSMENT," *Macroeconomic Dynamics*, 2016, *20* (5), 1313–1340.

Zivanovic, Jelena, "What Does Structural Analysis of the External Finance Premium Say About Financial Frictions?," Bank of Canada Staff Working Paper 2019-38, Bank of Canada 2019.

Appendix (For Online-Publication)

Appendix A Data

Our measurement equations contain eight variables:

- GDP: Δ ln(GDP/GDPDEF/CNP16OV)*100
- CONS: Δ ln((PCEC)/GDPDEF/CNP16OV)*100
- INV: Δ ln((FPI)/GDPDEF/CNP16OV)*100
- LAB: ln((AWHNONAG*CE16OV)/CNP16OV)*100
- INFL: Δ ln(GDPDEF)*100
- WAGE: Δ ln(COMPNFB/GDPDEF)*100
- FFR: FEDFUNDS/4
- BAA: (BAAspread)/4

For GDP, CONS, INV, INFL and WAGE we use the log changes in our measurement equations. We demean LAB in our measurement equation.

Data sources:

- GDP: Gross Domestic Product, Billions of Dollars, Quarterly, Seasonally Adjusted Annual Rate, FRED
- GDPDEF: Gross Domestic Product: Implicit Price Deflator, Index 2012=100, Quarterly, Seasonally Adjusted, FRED
- PCEC: Personal Consumption Expenditures, Billions of Dollars, Quarterly, Seasonally Adjusted Annual Rate, FRED
- FPI: Fixed Private Investment, Billions of Dollars, Quarterly, Seasonally Adjusted Annual Rate, FRED
- AWHNONAG: Average Weekly Hours of Production and Nonsupervisory Employees: Total private, Hours, Quarterly, Seasonally Adjusted, FRED.
- CE16OV: Civilian Employment Level, Thousands of Persons, Seasonally Adjusted, FRED.
- CNP16OV: trailing MA(5) of the Civilian Noninstitutional Population, Thousands of Persons, Quarterly, Not Seasonally Adjusted, FRED.

- COMPNFB, Nonfarm Business Sector: Compensation Per Hour, Index 2012=100, Quarterly, Seasonally Adjusted, FRED
- FEDFUNDS: Effective Federal Funds Rate, Percent, FRED.
- BAAspread: BAA Corportate Bond Yield Relative to Yield of 10-Year Treasury Constant Maturity, Percent, Not Seasonally Adjusted, FRED.

Appendix A.1 Data and further details for euro area estimation

- GDP: Δ ln(GDP/WAP)*100
- CONS: Δ ln(CONS/WAP)*100
- INV: Δ ln((GFCF-4*IP)/WAP)*100
- LAB: demeaned (ln(Hours*100/WAP)*100)
- INFL: Δ ln(GDPDEF)*100
- WAGE: Δ ln(Wage/Hours/GDPDEF)*100
- IOR: max(Euribor/4,0); NIRP: min(Euribor/4,0)
- GM: (GM-spread)/4

Data sources:

- GDP: EA19; Gross Domestic Product, constant prices, quarterly, seasonally adjusted, OECD
- CONS: EA19; Private Final Consumption Expenditures, constant prices, quarterly, seasonally adjusted, OECD
- GFCF: EA19; Gross Fixed Capital Formation, constant prices; quarterly, seasonally adjusted, OECD
- IP: EA19; Intellectual Property, constant prices; quarterly, seasonally adjusted, OECD
- Wage: EA19; Total Wages and Salaries, current prices, quarterly, seasonally adjusted, OECD
- Hours: EA19; Total Hours Worked, quarterly, seasonally adjusted, OECD
- GDPDEF: Gross Domestic Product, Price Index, OECD Reference Year, quarterly, seasonally adjusted, OECD
- WAP: Working Age Population (Age 15-64), Statistical Office of the European Communities

- Euribor: 3-months-rate, quarterly averages from monthly data, annualized, ECB
- GM-spread: Gilchrist-Mojon-Spread, quarterly averages from monthly data, annualized, Gilchrist and Mojon (2018)

To facilitate the nonlinear filtering, we assume small measurement errors for all variables with a variance that is 0.01 times the variance of the respective time series. Since the IOR+ and NIR rate are perfectly observable, we divide the measurement error variance here again by 100. Except for the labor supply, the data is not demeaned as we assume the non-stationary model follows a balanced growth path, with a growth rate estimated in line with SW.

We fix several parameters prior to estimating the others. In line with SW, let the depreciation rate be $\delta = 0.025$, the steady state government share in GDP to G/Y = 0.18, and the curvature parameters of the Kimball aggregators for prices and wages to $\epsilon_p = \epsilon_w = 10$. The steady state wage markup is set to $\lambda_w = 1.1$. Lastly, we calibrate the empirical perceived lower bound of the nominal interest rate to exactly to zero.

Appendix B Parameter estimates

	Prior			Posterior								
				RANK 1964–2019			RANK 1983–2019			RANK 1998–2019		
	distribution	mean	sd/df	mean	sd	mode	mean	sd	mode	mean	sd	mode
σ_c	normal	1.500	0.375	1.156	0.121	1.023	1.500	0.150	1.539	1.048	0.106	1.091
σ_l	normal	2.000	0.750	3.333	0.416	3.490	2.411	0.471	2.468	2.440	0.441	2.043
β_{tpr}	gamma	0.250	0.100	0.147	0.044	0.146	0.148	0.045	0.175	0.131	0.044	0.133
h	beta	0.700	0.100	0.635	0.042	0.667	0.590	0.054	0.560	0.523	0.052	0.415
S	normal	4.000	1.500	5.140	0.637	5.574	4.435	0.890	4.444	5.154	0.994	5.507
ι_p	beta	0.500	0.150	0.657	0.058	0.651	0.425	0.109	0.395	0.367	0.124	0.436
ι_w	beta	0.500	0.150	0.528	0.092	0.586	0.493	0.106	0.582	0.413	0.124	0.315
α	normal	0.300	0.050	0.173	0.015	0.157	0.213	0.017	0.222	0.191	0.019	0.206
ζ_p	beta	0.500	0.100	0.904	0.016	0.900	0.714	0.042	0.670	0.909	0.021	0.887
ζ_w	beta	0.500	0.100	0.817	0.018	0.823	0.773	0.051	0.743	0.815	0.156	0.619
Φ_p	normal	1.250	0.125	1.440	0.058	1.412	1.591	0.067	1.629	1.318	0.065	1.293
ψ	beta	0.500	0.150	0.502	0.077	0.460	0.617	0.083	0.685	0.840	0.055	0.851
ϕ_π	normal	1.500	0.250	2.190	0.128	2.198	1.958	0.164	1.987	2.229	0.415	2.536
ϕ_y	normal	0.125	0.050	0.173	0.018	0.194	0.072	0.029	0.054	0.085	0.024	0.078
ϕ_{dy}	normal	0.125	0.050	0.254	0.018	0.258	0.250	0.023	0.263	0.235	0.033	0.258
ρ	beta	0.750	0.100	0.870	0.012	0.876	0.820	0.027	0.804	0.904	0.026	0.868
ρ_r	beta	0.500	0.200	0.098	0.039	0.111	0.192	0.068	0.231	0.339	0.108	0.246
ρ_g	beta	0.500	0.200	0.949	0.017	0.939	0.972	0.010	0.968	0.940	0.018	0.937
ρ_z	beta	0.500	0.200	0.985	0.002	0.985	0.968	0.009	0.965	0.976	0.007	0.973
ρ_u	beta	0.500	0.200	0.836	0.022	0.845	0.499	0.141	0.486	0.910	0.011	0.908
ρ_p	beta	0.500	0.200	0.167	0.059	0.160	0.808	0.127	0.882	0.343	0.127	0.317
ρ_w	beta	0.500	0.200	0.990	0.003	0.986	0.936	0.030	0.942	0.700	0.288	0.988
ρ_i	beta	0.500	0.200	0.651	0.038	0.637	0.822	0.053	0.844	0.756	0.065	0.701
ρ_{fin}	beta	0.500	0.200	0.904	0.021	0.915	0.926	0.023	0.922	0.884	0.029	0.898
μ_p	beta	0.500	0.200	0.140	0.077	0.077	0.646	0.129	0.706	0.224	0.082	0.233
μ_w	beta	0.500	0.200	0.968	0.005	0.966	0.851	0.064	0.850	0.631	0.273	0.880
ρ_{gz}	normal	0.500	0.250	1.316	0.089	1.299	1.394	0.100	1.386	1.183	0.133	1.251
σ_g	inv.gamma	0.100	2.000	0.467	0.023	0.469	0.496	0.025	0.495	0.374	0.023	0.373
σ_u	inv.gamma	0.100	2.000	0.574	0.070	0.586	1.088	0.339	0.972	0.201	0.022	0.159
σ_z	inv.gamma	0.100	2.000	0.437	0.027	0.467	0.395	0.025	0.381	0.338	0.028	0.354
σ_r	inv.gamma	0.100	2.000	0.197	0.010	0.200	0.223	0.012	0.223	0.105	0.013	0.104
σ_p	inv.gamma	0.100	2.000	0.143	0.010	0.135	0.119	0.012	0.110	0.115	0.012	0.111
σ_w	inv.gamma	0.100	2.000	0.340	0.016	0.338	0.258	0.021	0.274	0.395	0.030	0.377
σ_i	inv.gamma	0.100	2.000	0.387	0.030	0.386	0.365	0.033	0.350	0.285	0.031	0.304
σ_{fin}	inv.gamma	0.100	2.000	0.079	0.003	0.078	0.080	0.004	0.083	0.078	0.004	0.076
$\overline{\gamma}$	normal	0.440	0.050	0.351	0.013	0.346	0.402	0.017	0.399	0.392	0.019	0.386
$\overline{l}$	normal	0.000	2.000	3.257	0.760	2.711	1.653	0.849	1.266	-3.650	1.150	-4.206
$\overline{\pi}$	gamma	0.625	0.100	0.936	0.097	0.986	0.973	0.084	0.979	0.885	0.201	1.035
$\overline{spread}$	normal	0.500	0.100	0.518	0.042	0.522	0.540	0.058	0.543	0.544	0.040	0.527

Table B.2: Estimation results for RANK

	Prior			Posterior								
				FRANK 1964–2019			FRANK 1983–2019			FRANK 1998–2019		
	distribution	mean	sd/df	mean	sd	mode	mean	sd	mode	mean	sd	mode
σ_c	normal	1.500	0.375	1.782	0.178	1.563	0.570	0.042	0.546	1.421	0.138	1.395
σ_l	normal	2.000	0.750	2.413	0.457	2.430	2.403	0.437	2.236	1.466	0.389	1.537
β_{tpr}	gamma	0.250	0.100	0.105	0.034	0.124	0.410	0.067	0.339	0.080	0.026	0.066
h	beta	0.700	0.100	0.357	0.044	0.364	0.761	0.031	0.776	0.292	0.040	0.297
S	normal	4.000	1.500	2.979	0.530	2.406	4.510	0.643	4.846	2.346	0.562	2.189
ι_p	beta	0.500	0.150	0.823	0.181	0.858	0.890	0.033	0.882	0.278	0.081	0.297
ι_w	beta	0.500	0.150	0.676	0.086	0.702	0.775	0.073	0.815	0.353	0.101	0.311
α	normal	0.300	0.050	0.133	0.017	0.134	0.147	0.017	0.152	0.150	0.017	0.158
ζ_p	beta	0.500	0.100	0.927	0.022	0.933	0.829	0.023	0.850	0.911	0.015	0.915
ζ_w	beta	0.500	0.100	0.940	0.011	0.944	0.915	0.015	0.921	0.830	0.028	0.824
Φ_p	normal	1.250	0.125	1.581	0.068	1.594	1.481	0.062	1.476	1.382	0.061	1.405
ψ	beta	0.500	0.150	0.479	0.099	0.566	0.439	0.092	0.491	0.784	0.072	0.835
ϕ_π	normal	1.500	0.250	1.195	0.046	1.168	1.035	0.022	1.051	1.461	0.197	1.519
ϕ_y	normal	0.125	0.050	0.013	0.012	0.009	-0.009	0.009	-0.014	0.138	0.018	0.146
ϕ_{dy}	normal	0.125	0.050	0.201	0.021	0.188	0.203	0.021	0.196	0.207	0.019	0.208
ρ	beta	0.750	0.100	0.741	0.027	0.723	0.742	0.024	0.745	0.886	0.025	0.879
ρ_r	beta	0.500	0.200	0.168	0.063	0.154	0.166	0.052	0.197	0.244	0.071	0.261
ρ_g	beta	0.500	0.200	0.993	0.004	0.993	0.867	0.030	0.889	0.964	0.009	0.966
ρ_z	beta	0.500	0.200	0.982	0.005	0.983	0.967	0.012	0.976	0.919	0.010	0.921
ρ_u	beta	0.500	0.200	0.976	0.005	0.972	0.977	0.005	0.979	0.969	0.006	0.972
ρ_p	beta	0.500	0.200	0.240	0.175	0.194	0.209	0.076	0.161	0.322	0.083	0.296
ρ_w	beta	0.500	0.200	0.414	0.095	0.439	0.481	0.119	0.445	0.131	0.058	0.098
ρ_i	beta	0.500	0.200	0.836	0.036	0.873	0.896	0.029	0.885	0.876	0.033	0.907
ρ_{fin}	beta	0.500	0.200	0.953	0.020	0.951	0.920	0.026	0.937	0.867	0.048	0.881
μ_p	beta	0.500	0.200	0.262	0.080	0.272	0.279	0.069	0.285	0.232	0.082	0.200
μ_w	beta	0.500	0.200	0.401	0.089	0.438	0.341	0.133	0.274	0.364	0.061	0.318
ρ_{gz}	normal	0.500	0.250	1.236	0.107	1.242	1.273	0.096	1.284	0.905	0.135	1.042
σ_g	inv.gamma	0.100	2.000	0.495	0.024	0.478	0.478	0.025	0.469	0.420	0.029	0.423
σ_u	inv.gamma	0.100	2.000	0.061	0.006	0.058	0.054	0.005	0.053	0.089	0.008	0.097
σ_z	inv.gamma	0.100	2.000	0.385	0.024	0.374	0.437	0.029	0.428	0.344	0.029	0.340
σ_r	inv.gamma	0.100	2.000	0.233	0.013	0.247	0.237	0.012	0.242	0.068	0.009	0.074
σ_p	inv.gamma	0.100	2.000	0.137	0.020	0.142	0.141	0.010	0.149	0.134	0.014	0.131
σ_w	inv.gamma	0.100	2.000	0.356	0.021	0.373	0.251	0.020	0.238	0.559	0.044	0.544
σ_i	inv.gamma	0.100	2.000	0.403	0.036	0.412	0.305	0.023	0.297	0.367	0.048	0.400
σ_{fin}	inv.gamma	0.100	2.000	0.066	0.003	0.065	0.060	0.003	0.059	0.071	0.007	0.072
$\overline{\gamma}$	normal	0.440	0.050	0.329	0.024	0.342	0.363	0.013	0.367	0.336	0.020	0.344
$\overline{l}$	normal	0.000	2.000	-2.154	1.175	-2.269	0.008	0.748	0.595	2.559	0.460	2.208
$\overline{\pi}$	gamma	0.625	0.100	0.810	0.129	0.813	0.600	0.082	0.582	0.703	0.051	0.723
$\overline{spread}$	normal	0.500	0.100	0.356	0.040	0.363	0.280	0.038	0.292	0.217	0.050	0.227
ζ_{spb}	beta	0.050	0.005	0.051	0.004	0.048	0.047	0.003	0.047	0.051	0.004	0.050

Table B.3: Estimation results for FRANK

	Prior			Posterior					
				RANK			FRANK		
	distribution	mean	sd/df	mean	sd	mode	mean	sd	mode
σ_c	normal	1.500	0.375	1.435	0.337	1.212	1.681	0.182	1.637
σ_l	normal	2.000	0.750	0.627	0.535	0.005	1.304	0.432	1.731
β_{tpr}	gamma	0.250	0.100	0.207	0.077	0.143	0.163	0.065	0.169
h	beta	0.700	0.100	0.607	0.087	0.647	0.602	0.058	0.557
S	normal	4.000	1.500	4.904	1.107	5.094	8.538	1.225	8.528
ι_p	beta	0.500	0.150	0.325	0.121	0.351	0.462	0.156	0.631
ι_w	beta	0.500	0.150	0.313	0.108	0.337	0.398	0.142	0.170
α	normal	0.300	0.050	0.272	0.020	0.256	0.300	0.020	0.280
ζ_p	beta	0.500	0.100	0.856	0.029	0.849	0.863	0.058	0.885
ζ_w	beta	0.500	0.100	0.777	0.063	0.714	0.847	0.051	0.907
Φ_p	normal	1.250	0.125	1.730	0.076	1.708	1.710	0.078	1.665
ψ	beta	0.500	0.150	0.307	0.069	0.281	0.378	0.062	0.371
ϕ_π	normal	1.500	0.250	1.653	0.255	1.744	1.849	0.263	1.217
ϕ_y	normal	0.125	0.050	0.220	0.032	0.202	0.185	0.042	0.246
ϕ_{dy}	normal	0.125	0.050	0.115	0.031	0.117	0.195	0.039	0.196
ρ	beta	0.750	0.100	0.919	0.026	0.913	0.909	0.023	0.891
ρ_r	beta	0.500	0.200	0.375	0.108	0.264	0.582	0.074	0.786
ρ_g	beta	0.500	0.200	0.966	0.015	0.964	0.955	0.019	0.965
ρ_z	beta	0.500	0.200	0.954	0.022	0.935	0.969	0.017	0.982
ρ_u	beta	0.500	0.200	0.962	0.016	0.954	0.983	0.021	0.989
ρ_p	beta	0.500	0.200	0.713	0.114	0.788	0.426	0.194	0.340
ρ_w	beta	0.500	0.200	0.744	0.085	0.762	0.692	0.108	0.682
ρ_i	beta	0.500	0.200	0.605	0.117	0.545	0.873	0.023	0.854
ρ_{fin}	beta	0.500	0.200	0.940	0.022	0.940	0.976	0.015	0.973
ρ_{nirp}	beta	0.500	0.200	0.984	0.007	0.986	0.981	0.010	0.988
μ_p	beta	0.500	0.200	0.733	0.132	0.818	0.408	0.185	0.470
μ_w	beta	0.500	0.200	0.518	0.165	0.515	0.503	0.172	0.560
ρ_{gz}	normal	0.500	0.250	1.117	0.150	1.164	1.123	0.163	1.192
σ_g	inv.gamma	0.100	0.250	0.234	0.024	0.204	0.235	0.020	0.235
σ_u	inv.gamma	0.100	0.250	0.176	0.051	0.178	0.077	0.016	0.061
σ_z	inv.gamma	0.100	0.250	0.217	0.024	0.236	0.218	0.024	0.197
σ_r	inv.gamma	0.100	0.250	0.080	0.012	0.078	0.081	0.012	0.061
σ_p	inv.gamma	0.100	0.250	0.147	0.018	0.146	0.132	0.018	0.148
σ_w	inv.gamma	0.100	0.250	0.108	0.018	0.101	0.118	0.020	0.104
σ_i	inv.gamma	0.100	0.250	0.328	0.056	0.323	0.309	0.037	0.306
σ_{fin}	inv.gamma	0.100	0.250	0.152	0.015	0.154	0.113	0.016	0.122
σ_{nirp}	inv.gamma	0.100	0.250	0.006	0.001	0.006	0.007	0.001	0.006
$\overline{\gamma}$	normal	0.440	0.050	0.297	0.025	0.275	0.350	0.037	0.303
$\overline{l}$	normal	0.000	2.000	3.082	0.736	3.545	4.135	0.937	3.916
$\overline{\pi}$	gamma	0.625	0.100	0.576	0.071	0.569	0.821	0.122	0.675
$\overline{spread}$	normal	0.500	0.100	0.355	0.097	0.306	0.408	0.065	0.351
ζ_{spb}	beta	0.050	0.005	–	–	–	0.049	0.005	0.050

Table B.4: Estimation results for the Euro Area 1998:I-2019:IV

Appendix C Model Descriptions

We adopt the framework by Smets and Wouters (2007) as a baseline model to interpret the Great Recession. Following Del Negro and Schorfheide (2013), we detrend all nonstationary variables by $Z_t = e^{\gamma t + \frac{1}{1-\alpha}\widetilde{z}_t}$, where, γ is the steady-state growth rate of the economy and α is the output share of capital. $\widetilde{z}_t$ is the linearly detrended log productivity process that follows the autoregressive law of motion $\widetilde{z}_t = \rho_z \widetilde{z}_{t-1} + \sigma_z \epsilon_z$. For z_t, the growth rate of technology in deviations from γ, it holds that $z_t = \frac{1}{1-\alpha}(\rho_z - 1)\widetilde{z}_t + \frac{1}{1-\alpha}\sigma_z \epsilon_z$.

In both models, labor is differentiated by unions with monopoly power that face nominal rigidities for their wage setting process. Intermediate good producers employ labor and capital services and sell their goods to final goods firms. Final good firms are monopolistically competitive and face nominal rigidities as in . The model further allows for exogenous government spending and features a monetary authority that sets the short-term nominal interest rate according to a monetary policy rule. In FRANK, we assume that frictionless financial intermediates collect funds from households. These funds are lent with a spread, which reflects default risk, to entrepreneurs, who use it together with their own equity to purchase physical capital. Physical capital in turn is rented out to intermediate good producers.

Appendix C.1 The linearized RANK model

This subsection briefly presents the linearized equilibrium conditions. A detailed derivation of the linearized equations is discussed e.g. in the appendix to Smets and Wouters (2007). All variables in this section are expressed as a log-deviation from their respective steady state values. The consumption Euler equation of the households is given by

$$\begin{aligned} c_t = \frac{h/\gamma}{(1+h/\gamma)}(c_{t-1} - z_t) + \frac{1}{1+h/\gamma}E_t[c_{t+1} + z_{t+1}] + \frac{(\sigma_c - 1)(W^h L/C)}{\sigma_c(1+h/\gamma)}(l_t - E_t[l_{t+1}]) \\ - \frac{(1-h/\gamma)}{(1+h/\gamma)\sigma_c}(r_t - E_t[\pi_{t+1}] + u_t), \end{aligned} \tag{C.1}$$

where c_t is consumption, and l_t is their supply of labor. Parameters h, σ_c and σ_l are, respectively, the degree of external habit formation in consumption, the coefficient of relative risk aversion, and the inverse of the Frisch elasticity. γ denotes the steady-state growth rate of the economy. r_t is the nominal interest rate, π_t is the inflation rate, and u_t is an exogenous risk premium shock, which drives a wedge between the lending/savings rate and the riskless real rate.

Equation (C.2) is the linearized relationship between investment and the relative price of capital,

$$i_t = \frac{1}{1+\overline{\beta}}[(i_{t-1} - z_t] + \frac{\overline{\beta}}{1+\overline{\beta}}E_t[i_{t+1} + z_{t+1}] + \frac{1}{(1+\overline{\beta})\gamma^2 S''}q_t + v_{i,t}. \tag{C.2}$$

Here, i_t denotes investment in physical capital and q_t is the price of capital. It holds that $\overline{\beta} = \beta\gamma^{(1-\sigma_c)}$ where β is the households' discount factor. Investment is subject to adjustment costs, which are governed by S'', the steady-state value of the second derivative of the investment adjustment cost function, and an exogenous process, $v_{i,t}$. While Smets and Wouters (2007) interpret $e_{i,t}$ as an investment specific technology disturbance, Justiniano et al. (2011) stress that this shock can also be viewed as a reduced-form way of capturing financial frictions, as it drives a wedge between aggregate savings and aggregate investment. We henceforth refer to this disturbance as a shock on the marginal efficiency of investment (MEI).

The accumulation equation of physical capital is given by

$$\overline{k}_t = (1-\delta)/\gamma(\overline{k}_{t-1} - z_t) + (1-(1-\delta)/\gamma)i_t + (1-(1-\delta)/\gamma)(1+\overline{\beta})\gamma^2 S'' v_{i,t}, \tag{C.3}$$

where $\overline{k}$ denotes physical capital, and parameter δ is the depreciation rate. The following Equation (C.4) is the no-arbitrage condition between the rental rate of capital, r_t^k, and the riskless real rate:

$$r_t - E_t[\pi_{t+1}] + u_t = \frac{r^k}{r^k + (1-\delta)} E_t[r_{t+1}^k] + \frac{(1-\delta)}{r^k + (1-\delta)} E_t[q_{t+1}] - q_t. \tag{C.4}$$

As the use of physical capital in production is subject to utilization costs, which in turn can be expressed as a function of the rental rate on capital, the relation between the effectively used amount of capital k_t and the physical capital stock is

$$k_t = \frac{1-\psi}{\psi} r_t^k + \overline{k}_{t-1}, \tag{C.5}$$

where $\psi \in (0,1)$ is the parameter governing the costs of capital utilization. Equation (C.6) is the aggregate production function

$$y_t = \Phi(\alpha k_t + (1-\alpha)l_t + z_t) + (\Phi - 1)\frac{1}{1-\alpha}\widetilde{z}_t. \tag{C.6}$$

Intermediate good firms employ labor and capital services. Let z_t be the exogenous process of total factor productivity. Parameter α is the elasticity of output with respect to capital and Φ enters the production function due to the assumption of a fixed cost in production. Real marginal costs for producing firms, mc_t, can be written as

$$mc_t = w_t - z_t + \alpha(l_t - k_t). \tag{C.7}$$

w_t denotes the real wage, which are set by labor unions. Furthermore, cost minimization for

intermediate good producers results in condition (C.8):

$$k_t = w_t - r_t^k + l_t. \tag{C.8}$$

The aggregate resource constraint (C.9) contains an exogenous demand shifter, g_t, which comprises exogenous variations in government spending and net exports, as well as the resource costs of capital utilization:

$$y_t = \frac{G}{Y} g_t + \frac{C}{Y} c_t + \frac{I}{Y} i_t + \frac{R^k K}{Y} \frac{1-\psi}{\psi} r_t^k + \frac{1}{1-\alpha} \widetilde{z}_t.. \tag{C.9}$$

Final good producers are assumed to have monopoly power and face nominal rigidities as in Calvo (1983) when setting their prices. This gives rise to a New Keynesian Phillips Curve (NKPC) of the form

$$\pi_t = \frac{\overline{\beta}}{1 + \imath_p \overline{\beta}} E_t \pi_{t+1} + \frac{\imath_p}{1 + \imath_p \overline{\beta}} \pi_{t-1} + \frac{(1 - \zeta_p \overline{\beta})(1 - \zeta_p)}{(1 + \overline{\beta} \imath_p) \zeta_p ((\Phi - 1)\epsilon_p + 1)} mc_t + v_{p,t}. \tag{C.10}$$

Here, ζ_p is the probability that a firm cannot update its price in any given period. In addition to Calvo pricing, we assume partial price indexation, governed by the parameter $\imath_p$. The Phillips Curve is hence both, forward and backward looking. ϵ_p denotes the curvature of the Kimball (1995) aggregator for final goods. Due to the Kimball aggregator, the sensitivity of inflation to fluctuations in marginal cost is affected by the market power of firms, represented by the steady state price markup, $\Phi - 1$.[16] Furthermore, the curvature of the Kimball aggregator affects the adjustment of prices to marginal cost as the higher ϵ_p, the higher is the degree of strategic complementarity in price setting, dampening the price adjustment to shocks. The last term in the NKPC, $v_{p,t}$, represents exogenous fluctuations in the price markup.

While final good producers set prices on the good market, wages are set by labor unions. Unions bundle labor services from households and offer them to firms with a markup over the frictionless wage, w_t^h, which reads

$$w_t^h = \frac{1}{(1-h)} (c_t - h/\gamma c_{t-1} + h/\gamma z_t.) + \sigma_l l_t. \tag{C.11}$$

As with price setting, we assume that the nominal rigidities in the wage setting process are of the

[16] Note that in equilibrium, the steady state price markup is tied to the fixed cost parameter by a zero profit condition.

Calvo type, and include partial wage indexation. The wage Phillips curve is thus

$$w_t = \frac{1}{1+\bar{\beta}\gamma}(w_{t-1} - z_t + \imath_w \pi_{t-1}) + \frac{\bar{\beta}\gamma}{1+\bar{\beta}\gamma} E_t[w_{t+1} + z_{t+1} + \pi_{t+1}] - \frac{1+\imath_w\bar{\beta}\gamma}{1+\bar{\beta}\gamma}\pi_t + \frac{(1-\zeta_w\bar{\beta}\gamma)(1-\zeta_w)}{(1+\bar{\beta}\gamma)\zeta_w((\lambda_w-1)\epsilon_w+1)}(w_t^h - w_t) + v_{w,t}. \tag{C.12}$$

The term $w_t^h - w_t$ is the inverse of the wage markup. As in Equation (C.10), the terms λ_w and ϵ_w are the steady state wage markup and the curvature of the Kimball aggregator for labor services, respectively. The term $v_{w,t}$ represents exogenous variations in the wage markup.

We take into account the fact that the central bank is constrained in its interest rate policy by a lower bound (ELB) on the nominal interest rate. Therefore, in the linear model, it is that

$$r_t = \max\{\bar{r}, r_t^n\}, \tag{C.13}$$

with $\bar{r}$ being the lower bound value. Whenever the policy rate is away from the constraint, it corresponds to the notational rate, r_t^n, which follows the feedback rule

$$r_t^n = \rho r_{t-1}^n + (1-\rho)\left(\phi_\pi \pi_t + \phi_y \widetilde{y}_t\right) + \phi_{dy}\Delta\widetilde{y}_t + v_{r,t}. \tag{C.14}$$

Here, $\widetilde{y}_t$ is the output gap and $\Delta\widetilde{y}_t = \widetilde{y}_t - \widetilde{y}_{t-1}$ its growth rate. Parameter ρ expresses an interest rate smoothing motive by the central bank. ϕ_π, ϕ_y and ϕ_{dy} are feedback coefficients. When the economy is away from the ELB, the stochastic process $v_{r,t}$ represents a regular interest rate shock. When the nominal interest rate is zero, however, $v_{r,t}$ may not directly affect the level of the nominal interest rate. However, through the persistence of the stochastic process that drives $v_{r,t}$, it affects the expected path of the notational rate and can therefore alter the expected duration of the lower bound spell. It can hence be viewed as a forward guidance shock whenever the economy is at the ELB.

The model is augmented with an additional equation to allow for an estimation on the same observables as the FRANK model, including the spread. The equations simply reads

$$spread = \widetilde{\sigma}_{\omega,t},$$

where the variable 'spread' is unrelated to the dynamics of the rest of the model and is driven exclusively by the exogenous shock, $\widetilde{\sigma}_{\omega,t}$.

Finally, the stochastic drivers in our model are the following seven processes:

$$u_t = \rho_u u_{t-1} + \epsilon_t^u, \tag{C.15}$$

$$z_t = \rho_z z_{t-1} + \epsilon_t^z, \tag{C.16}$$

$$g_t = \rho_g g_{t-1} + \epsilon_t^g + \rho_{gz}\epsilon_t^z, \tag{C.17}$$

$$v_{r,t} = \rho_r v_{r,t-1} + \epsilon_t^r, \tag{C.18}$$

$$v_{i,t} = \rho_i v_{i,t-1} + \epsilon_t^i, \tag{C.19}$$

$$v_{p,t} = \rho_p v_{p,t-1} + \epsilon_t^p - \mu_p \epsilon_{t-1}^p, \tag{C.20}$$

$$v_{w,t} = \rho_w v_{w,t-1} + \epsilon_t^w - \mu_w \epsilon_{t-1}^w, \tag{C.21}$$

$$\widetilde{\sigma}_{\omega,t} = \rho_{fin}\widetilde{\sigma}_{\omega,t-1} + \epsilon_t^{\widetilde{\sigma}_\omega} \tag{C.22}$$

where $\epsilon_t^k \overset{iid}{\sim} N(0, \sigma_k^2)$ for all $k = \{r, i, p, w\}$, and likewise for $\{u_t, z_t, g_t, \widetilde{\sigma}_{\omega,t}\}$.

Appendix C.2 Financial Frictions

This subsection lays out the extension of the model: the inclusion of frictions in financial markets. Here, we adopt the modeling choices of Del Negro et al. (2015), who build on the work of Bernanke et al. (1999), and Christiano et al. (2014).

In this model, entrepreneurs obtain loans from frictionless financial intermediates, which in turn receive their funds from household at the riskless interest rate. In addition to the loans, entrepreneurs use their own net worth to finance the purchase of physical capital that they rent out to intermediate good producers. Entrepreneurs are subject to idiosyncratic shocks to their success in managing capital. As a consequence, their revenue might fall short of the amount needed to repay the loan, in which case they will default on their loan. In anticipation of the risk of entrepreneurs' default, financial intermediates pool their loans and charge a spread on the riskless rate to cover the expected losses arising from defaulting entrepreneurs. Therefore, in the full model, condition (C.4) in the RANK model is replaced by the two conditions

$$E_t[\widetilde{r}_{t+1}^k - r_t] = u_t + \zeta_{sp,b}(q_t + \overline{k}_t - n_t) + \widetilde{\sigma}_{\omega,t}, \tag{C.23}$$

$$\widetilde{r}_t^k - \pi_t = \frac{r^k}{r^k + (1-\delta)} r_t^k + \frac{(1-\delta)}{r^k + (1-\delta)} q_{t+1} - q_{t-1}. \tag{C.24}$$

$\widetilde{r}_t^k$ is the nominal return on capital for entrepreneurs, n_t denotes entrepreneurs' aggregate net worth, and $\widetilde{\sigma}_{\omega,t}$ allows for exogenous variations in the entrepreneurs' riskiness. The first condition defines the spread as a function of the entrepreneurs' leverage and their riskiness, which is determined by the dispersion of the idiosyncratic shocks to entrepreneurs. Note that if the elasticity of the loan rate to the entrepreneurs' leverage, $\zeta_{sp,b}$, is set to zero, we are back to the case without financial

frictions. Condition (C.24) defines the return on capital for entrepreneurs.

The evolution of aggregate entrepreneurial net worth is described by

$$n_t = \zeta_{n,\widetilde{r}^k}(\widetilde{r}^k_t - \pi_t) - \zeta_{n,r}(r_{t-1} - \pi_t) + \zeta_{n,qk}(q_{t-1} + \bar{k}_{t-1}) + \zeta_{n,n} n_{t-1} - \frac{\zeta_{n,\sigma_\omega}}{\zeta_{sp,\sigma_\omega}} \widetilde{\sigma}_{\omega,t-1} - \gamma_* \frac{\nu_*}{n_*} \widetilde{z}_t. \tag{C.25}$$

Equation (C.25) links the accumulated stock of entrepreneurial net worth to the real return of renting out capital to firms, the riskless real rate, its capital holdings, its past net worth and variations in riskiness. The coefficients $\zeta_{n,\widetilde{r}^k}$, $\zeta_{n,r}$, $\zeta_{n,qk}$, ζ_{n,σ_ω}, and ζ_{sp,σ_ω} are derived as in Del Negro et al. (2015). They depend on the steady state calibration of the default rate of entrepreneurs, the distribution of entrepreneurial risk, and their survival probability.

Lastly, the evolution of exogenous variations in entrepreneurial risk, the *risk shock* in terms of Christiano et al. (2014), follows the process

$$\widetilde{\sigma}_{\omega,t} = \rho_\sigma \widetilde{\sigma}_{\omega,t-1} + \epsilon_{\sigma,t}, \tag{C.26}$$

with $\epsilon_{\sigma,t} \overset{iid}{\sim} N(0, \sigma^2_\sigma)$.

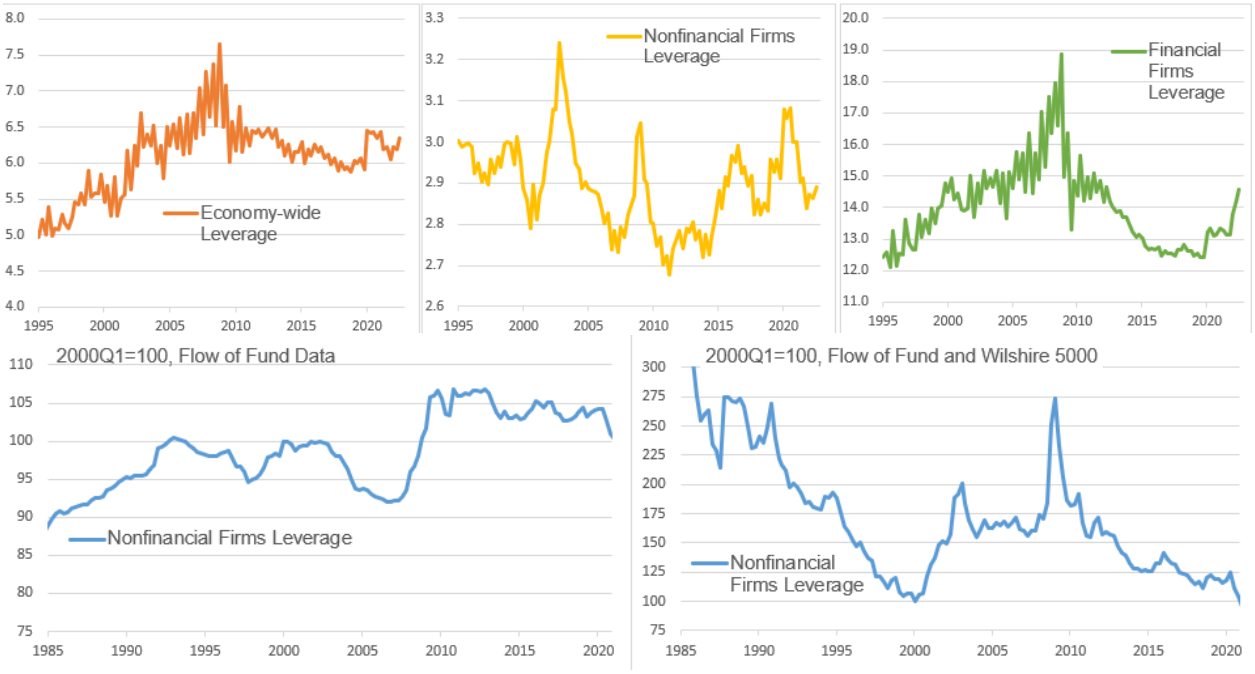

Figure D.8: Leverage ratios in the Great Recession in the US. Upper panels: aggregate asset-to-equity ratios of publicly listed US firms based on Compustat data (not seasonally adjusted). Lower-left panel: aggregate asset-to-equity ratio of non-financial US firms (corporate and non-corporate) based on flow-of-funds data. Lower-right panel: aggregate asset-to-equity ratio of non-financial US firms (corporate and non-corporate) using asset data from the flow-of-funds and using the Wilshire 5000 stocks index to proxy dynamics of equity.

Appendix D Leverage ratios in the Great Recession

Our estimated FRANK model implies a gradual build-up of the aggregate leverage ratio of US firms in the run-up to the Global Financial Crisis and a sizable deleveraging thereafter (cf. Figure 3). This broadly corresponds to the dynamics of the aggregate asset-to-equity ratio of publicly listed US firms calculated from balance sheet data provided by S&P Global in its Compustat dataset (see, Figure D.8, upper left panel).[17] This first-pass comparison provides a sanity check of our model and provides some credence to our results. In particular, this evidence for a falling leverage ratio of US firms taken together with the elevated credit spread after the financial crisis emphasizes the model's difficulties to explain the events after the GFC.

Figure D.8 also shows that any closer comparison between the model-implied leverage ratio and the trajectory of an empirical measure of the leverage ratio should be taken with a grain of salt. As we illustrate, there are various other measures that can be chosen to stand in for the US leverage ratio. Choosing the appropriate measure to be used in the context of a macroeconomic model is not straightforward. In the context of the BGG model, the focus is often on non-financial

[17] Calculated as sum of all assets (ATQ) divided by the sum of stockholders' equity (SEQQ) of all firms in Compustat.

firms. Balance-sheet data of listed non-financial US firms implies several sharp swings of the asset-to-equity ratio in the last decades.[18] Other data sources paint very different pictures of the asset-to-equity ratio of US nonfinancial firms. The lower-left panel of Figure D.8 shows the asset-to-equity ratio based on Flow-of-Funds data (corporate and non-corporate non-financial firms). Here, the image emerges of an upward trend of this variable in the 80s and 90s, a decline prior to the financial crisis, and a sharp increase during the GFC followed by a persistently elevated leverage ratio. Again, the picture changes, if, following Christiano et al. (2014), one replaces the dynamics of Flow-of-Funds net worth with those of the Wilshire 5000 stock index.[19] This results in a downward trend in the 80s and 90s, and sharp, short-lived spike in the GFC, followed by a deleveraging in the decade thereafter.

Given the very different dynamics of these measures and the potential implications for the estimation of a macro-financial model, we avoid including financial quantities in our estimation. This way, we circumvent the issue of selecting the "correct" financial quantities. Instead, our focus lies on the performance of standard models in explaining macroeconomic dynamics. For this end, restricting the set of observables to macroeconomic variables is preferable. It avoids the issue that the likelihood is driven by matching non-macroeconomic time series and it makes a direct comparison with models easier that do not allow financial variables.

[18]Here, non-financial firms are all firms except those, whose NAICS Code starts with the digits 52. The latter include banks, insurances, brokers and other financial institutes.

[19]Christiano et al. (2014) use credit market debt of US non-financial firms, not their assets. However, the implied leverage ratio displays very similar dynamics as the asset-to-equity ratio.

Appendix E The shape of the posterior distribution

The figures in this section show the 200 chains used for the estimation of the RANK model (E.9 to E.15) as well as the FRANK model (E.16 to E.22). See Boehl (2022b) for details on the differential independence mixture ensemble (DIME) Monte Carlo Marcov chain method we use for posterior sampling. For each model, we run a total of 2500 iterations, of which we keep the last 500. That means that the posterior contains $500 \times 200 = 10,000$ parameter draws. We check for convergence using the method of integrated autocorrelation time with a window size of $c = 50$, as suggested by Goodman and Weare (2010). Note that it is not trivial to find a sufficient statistics for convergence since the samples in the chain are not independent. The figures strongly suggest that the estimation of the RANK model is converged from iteration 2000 onwards. For the FRANK model, convergence sets in somewhat later, but is achieved within the burn-in period as well.

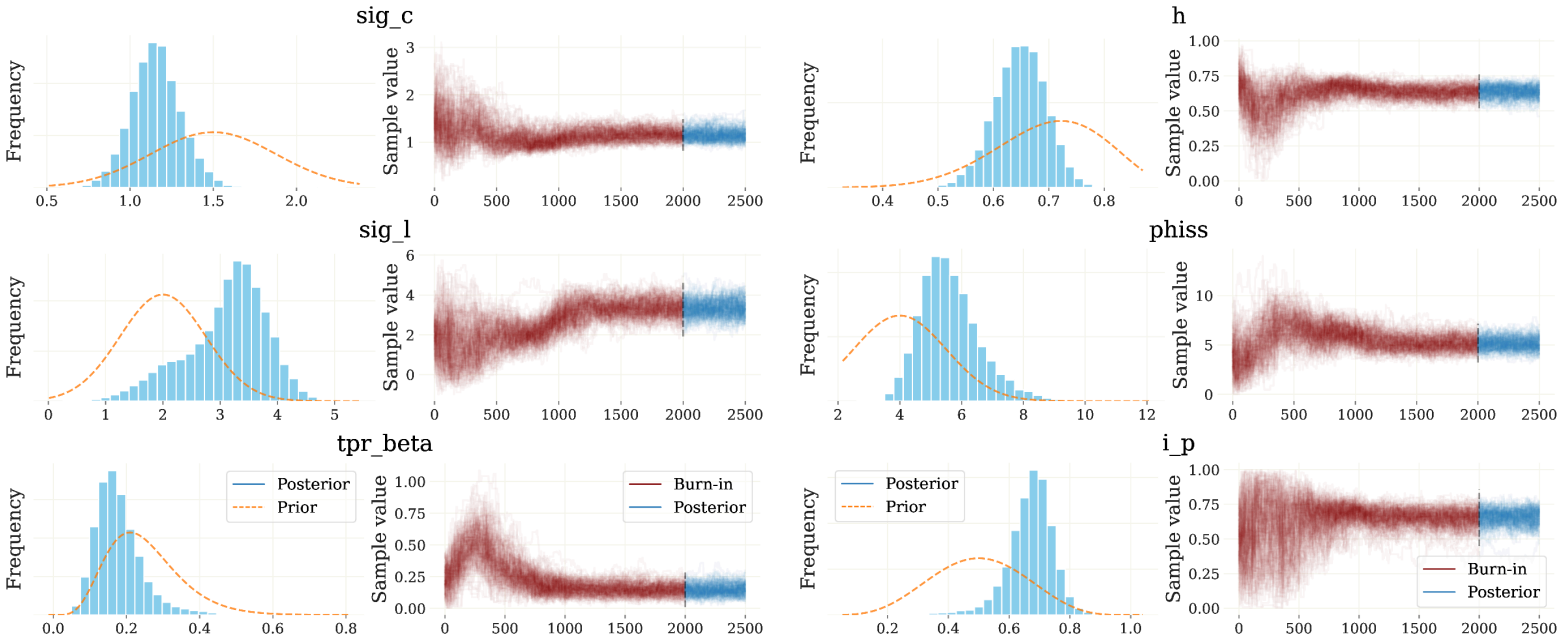

Figure E.9: Traceplots of the 200 DIME chains for selected parameters. Estimation of the RANK model. The left panel shows a KDE of the parameter distribution. The right displays the trace of each of the chains over time.

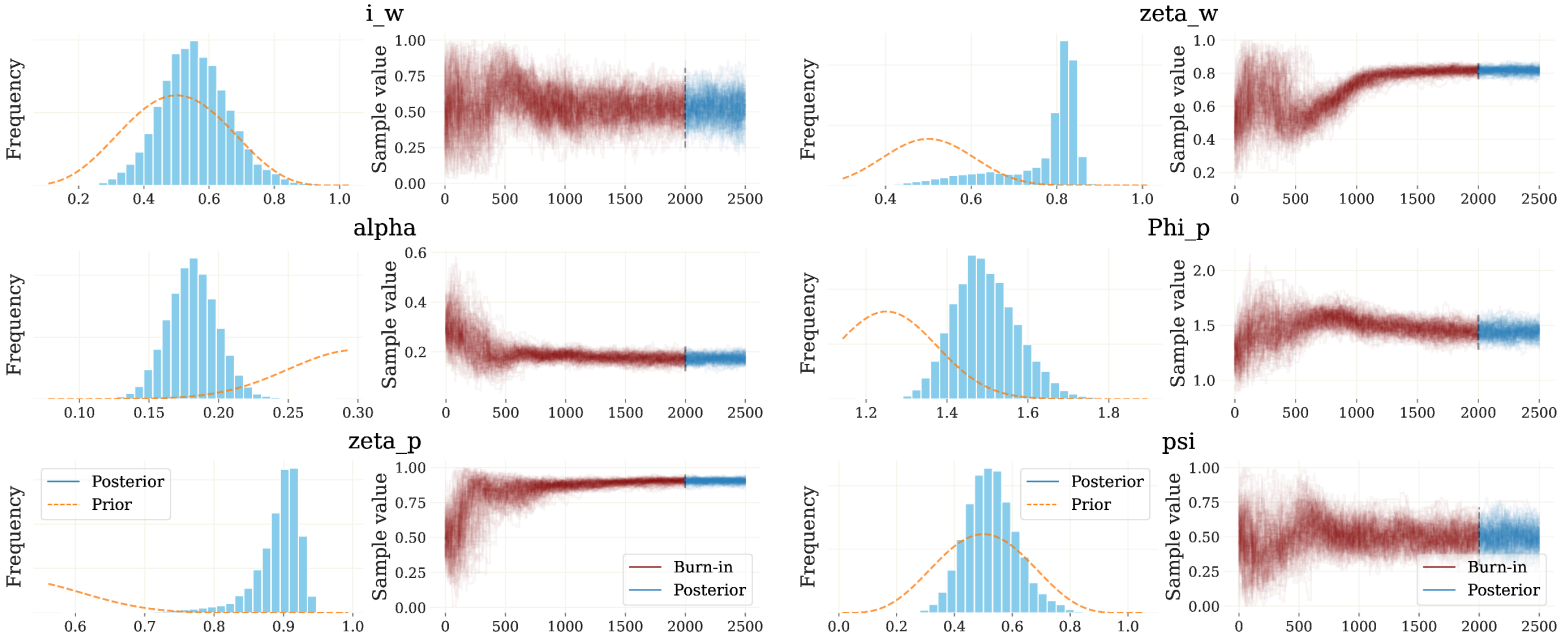

Figure E.10: Traceplots of the 200 DIME chains for selected parameters. Estimation of the RANK model. The left panel shows a KDE of the parameter distribution. The right displays the trace of each of the chains over time.

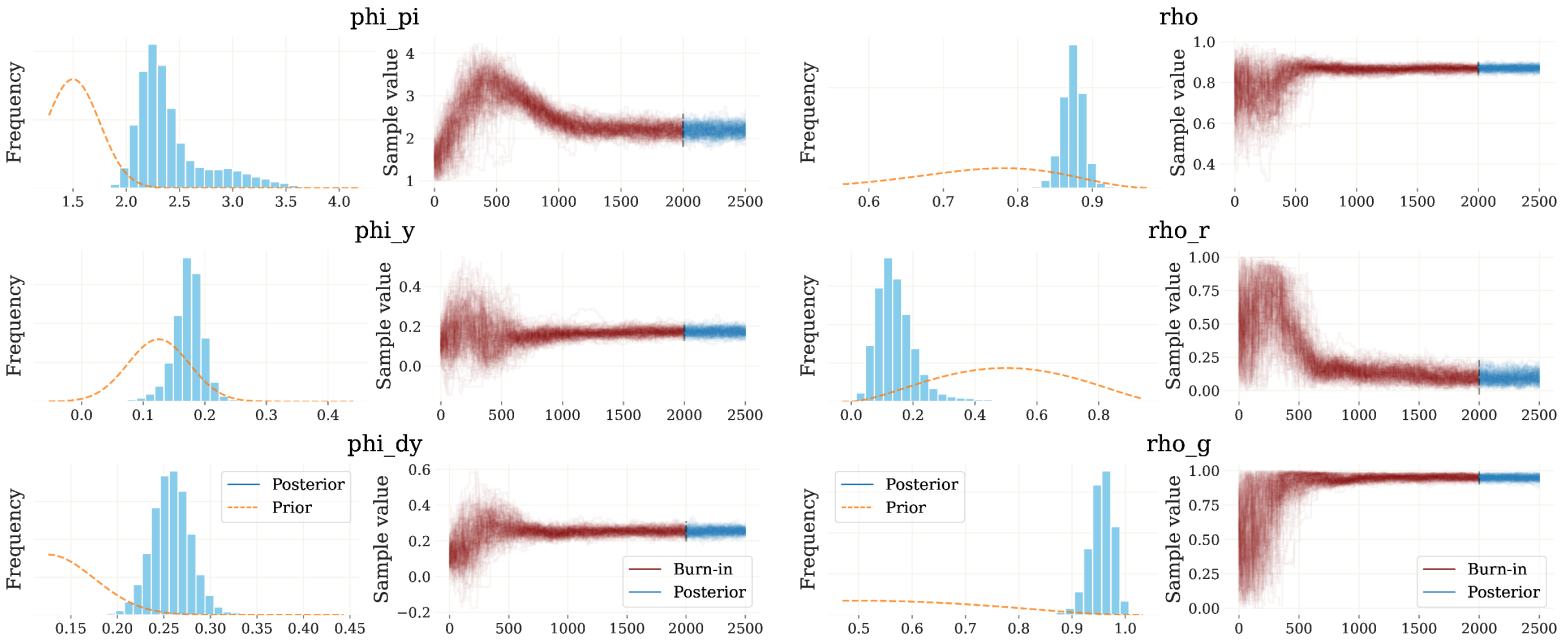

Figure E.11: Traceplots of the 200 DIME chains for selected parameters. Estimation of the RANK model. The left panel shows a KDE of the parameter distribution. The right displays the trace of each of the chains over time.

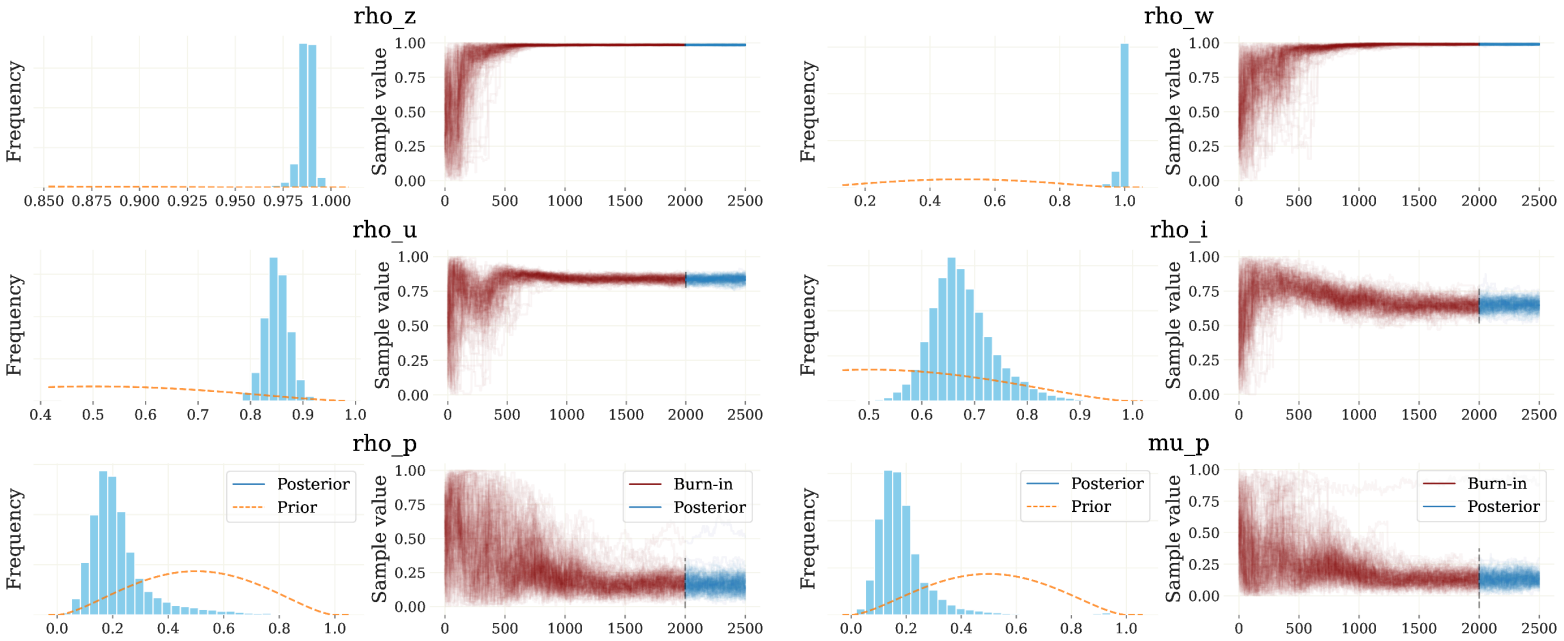

Figure E.12: Traceplots of the 200 DIME chains for selected parameters. Estimation of the RANK model. The left panel shows a KDE of the parameter distribution. The right displays the trace of each of the chains over time.

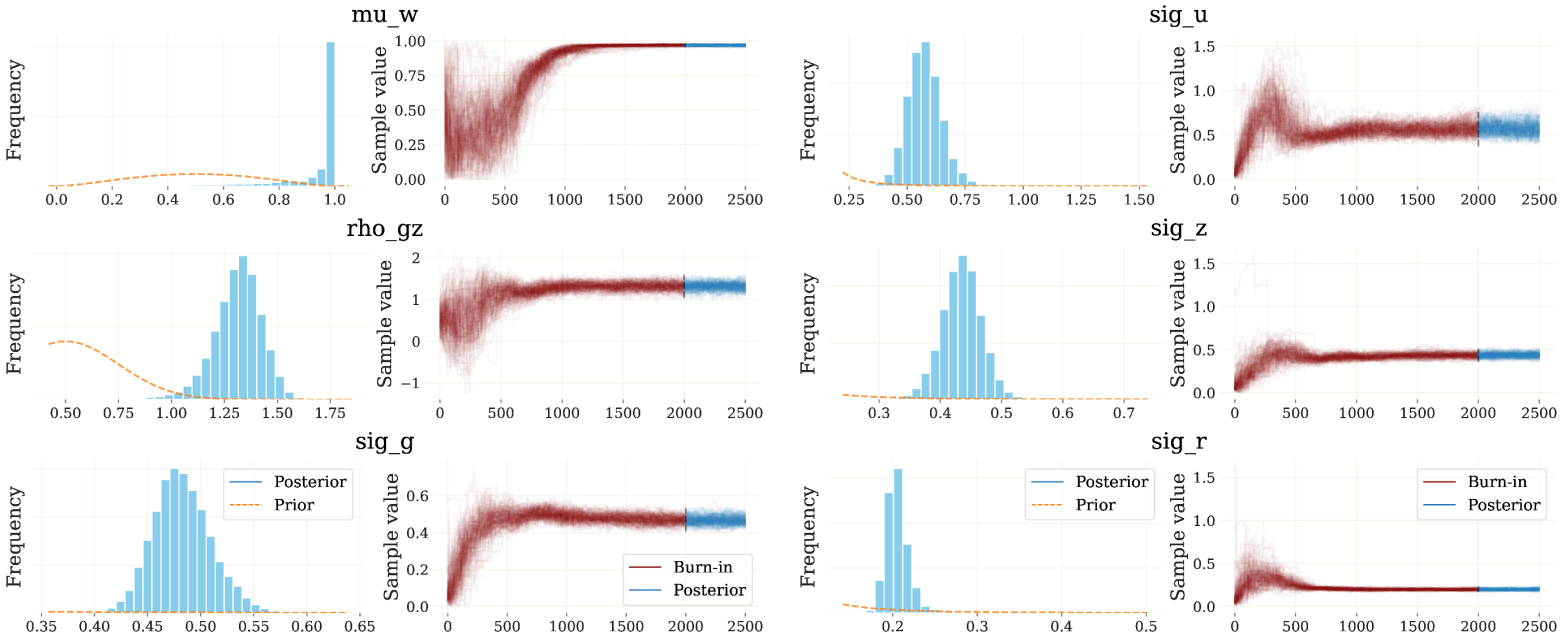

Figure E.13: Traceplots of the 200 DIME chains for selected parameters. Estimation of the RANK model. The left panel shows a KDE of the parameter distribution. The right displays the trace of each of the chains over time.

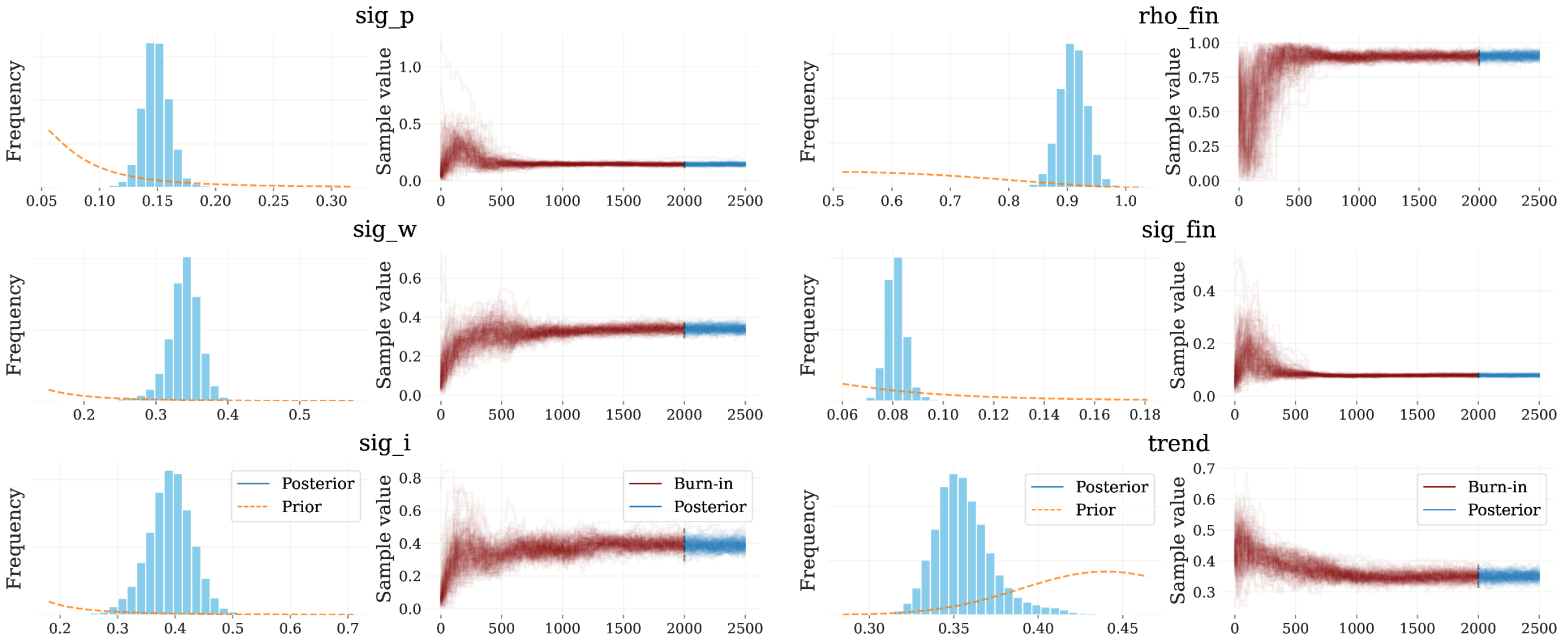

Figure E.14: Traceplots of the 200 DIME chains for selected parameters. Estimation of the RANK model. The left panel shows a KDE of the parameter distribution. The right displays the trace of each of the chains over time.

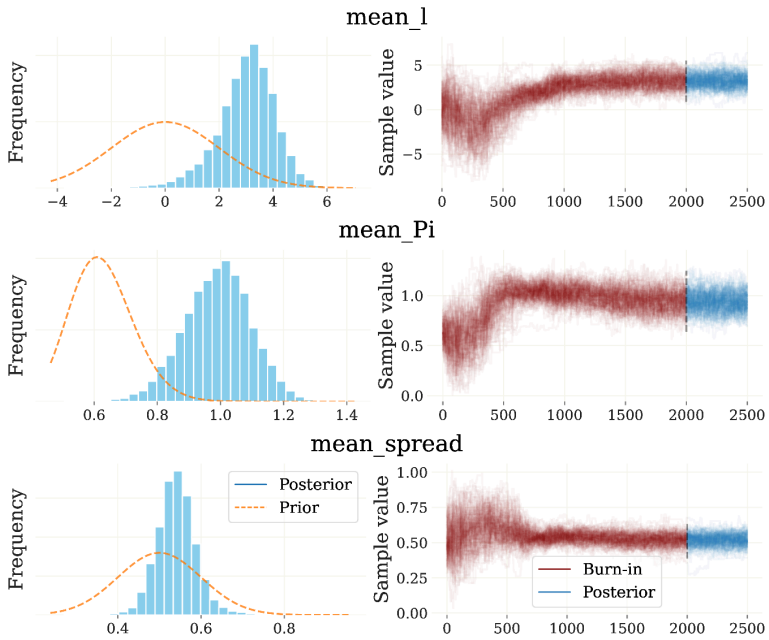

Figure E.15: Traceplots of the 200 DIME chains for selected parameters. Estimation of the RANK model. The left panel shows a KDE of the parameter distribution. The right displays the trace of each of the chains over time.

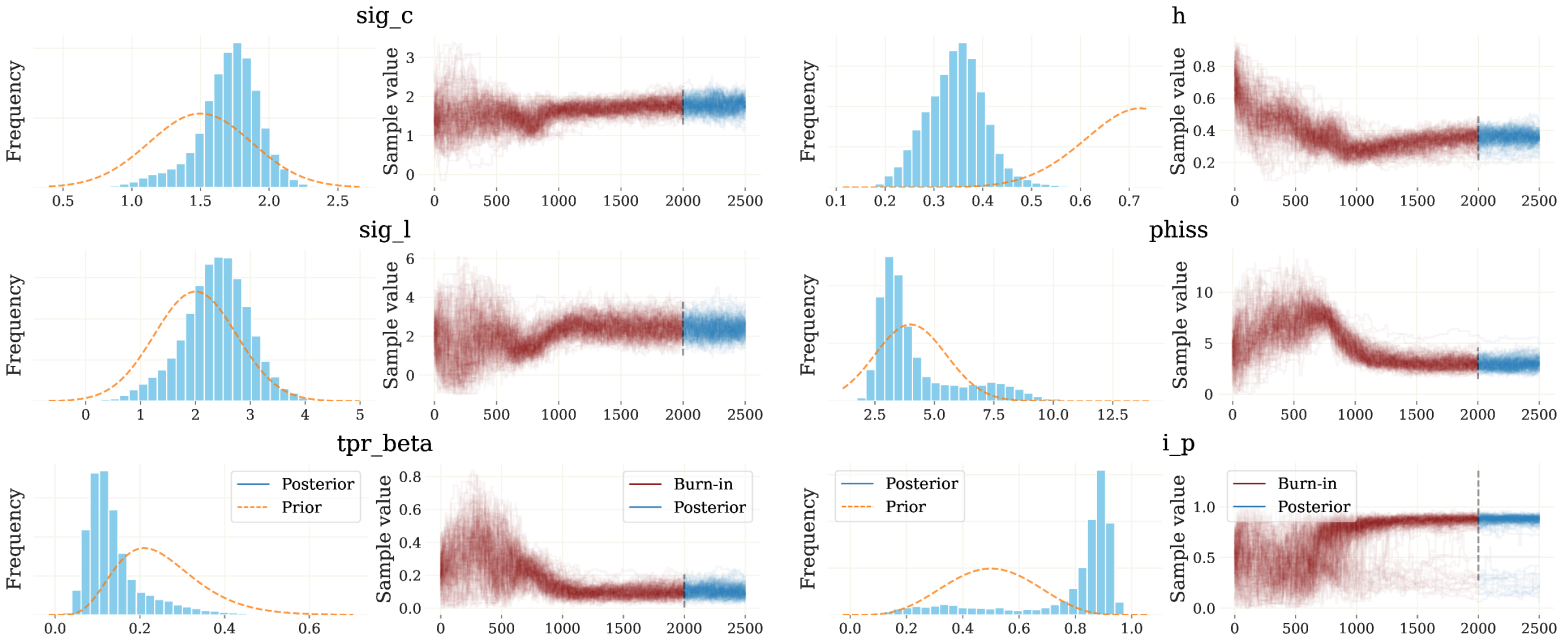

Figure E.16: Traceplots of the 200 DIME chains for selected parameters. Estimation of the FRANK model. The left panel shows a KDE of the parameter distribution. The right displays the trace of each of the chains over time.

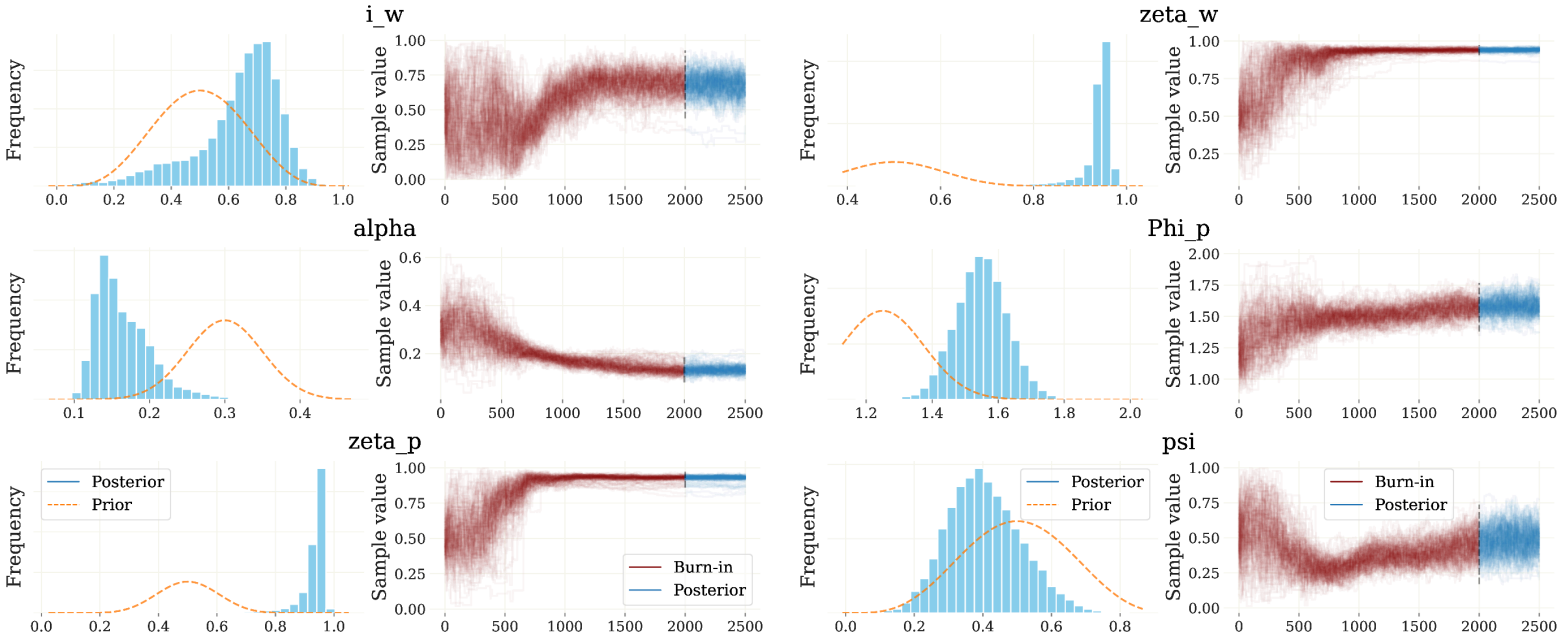

Figure E.17: Traceplots of the 200 DIME chains for selected parameters. Estimation of the FRANK model. The left panel shows a KDE of the parameter distribution. The right displays the trace of each of the chains over time.

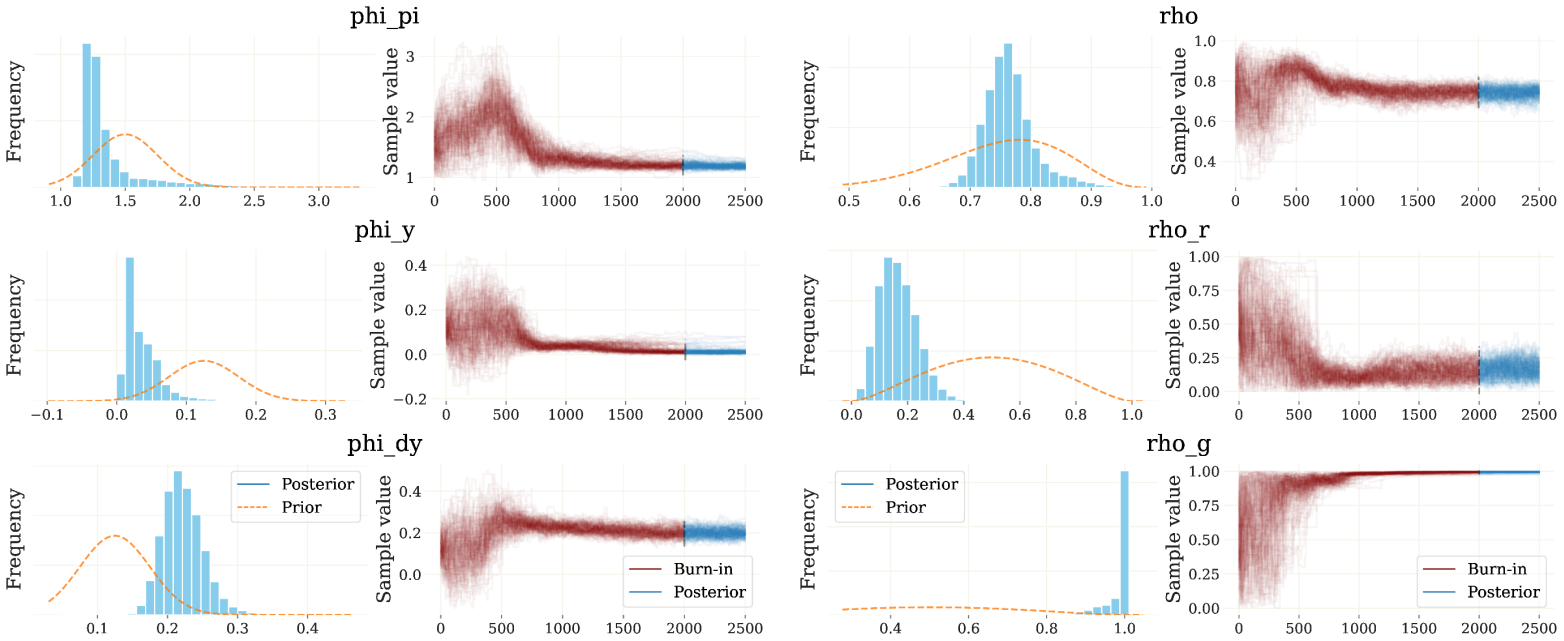

Figure E.18: Traceplots of the 200 DIME chains for selected parameters. Estimation of the FRANK model. The left panel shows a KDE of the parameter distribution. The right displays the trace of each of the chains over time.

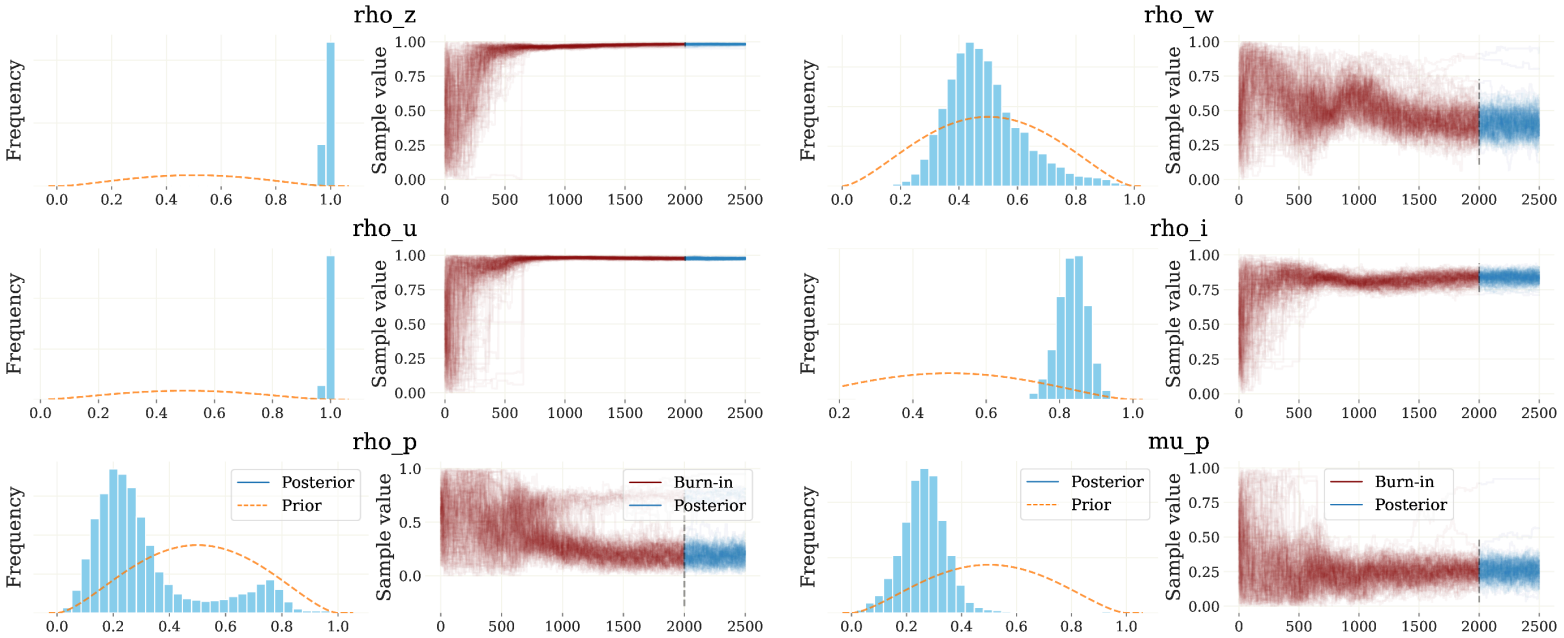

Figure E.19: Traceplots of the 200 DIME chains for selected parameters. Estimation of the FRANK model. The left panel shows a KDE of the parameter distribution. The right displays the trace of each of the chains over time.

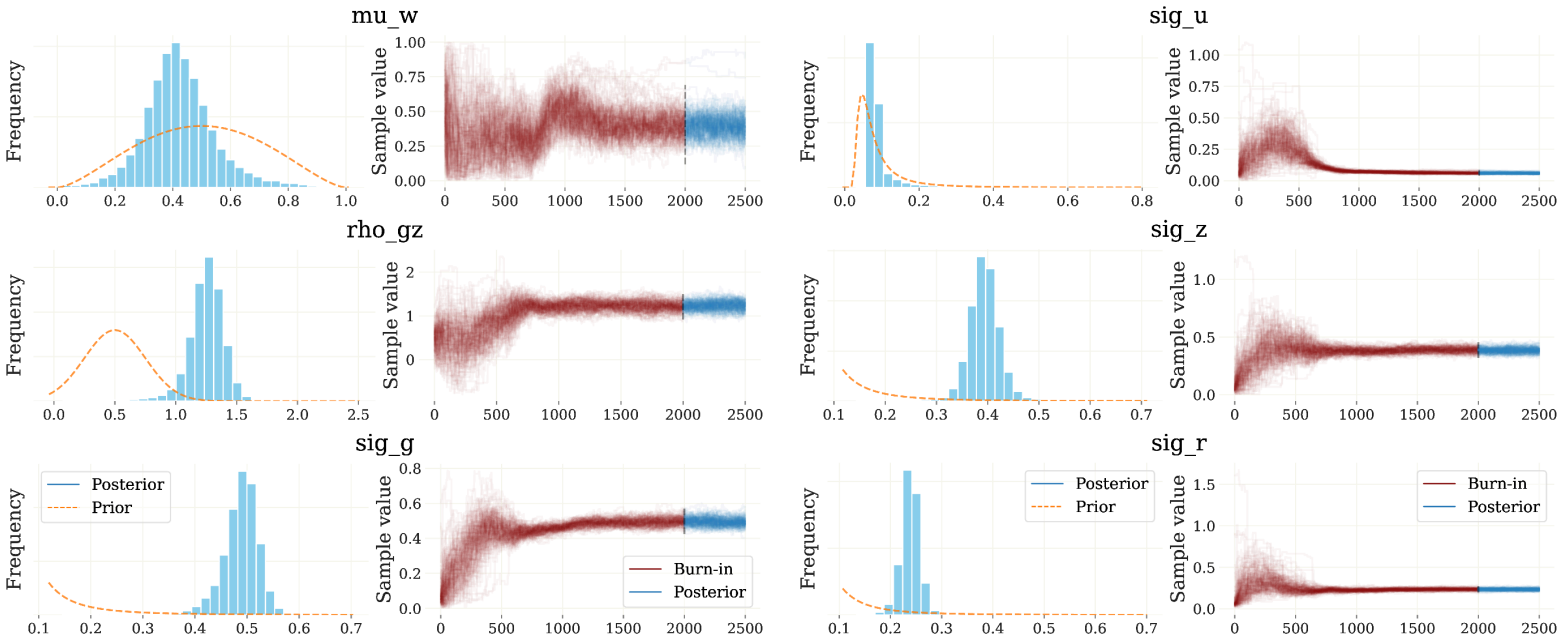

Figure E.20: Traceplots of the 200 DIME chains for selected parameters. Estimation of the FRANK model. The left panel shows a KDE of the parameter distribution. The right displays the trace of each of the chains over time.

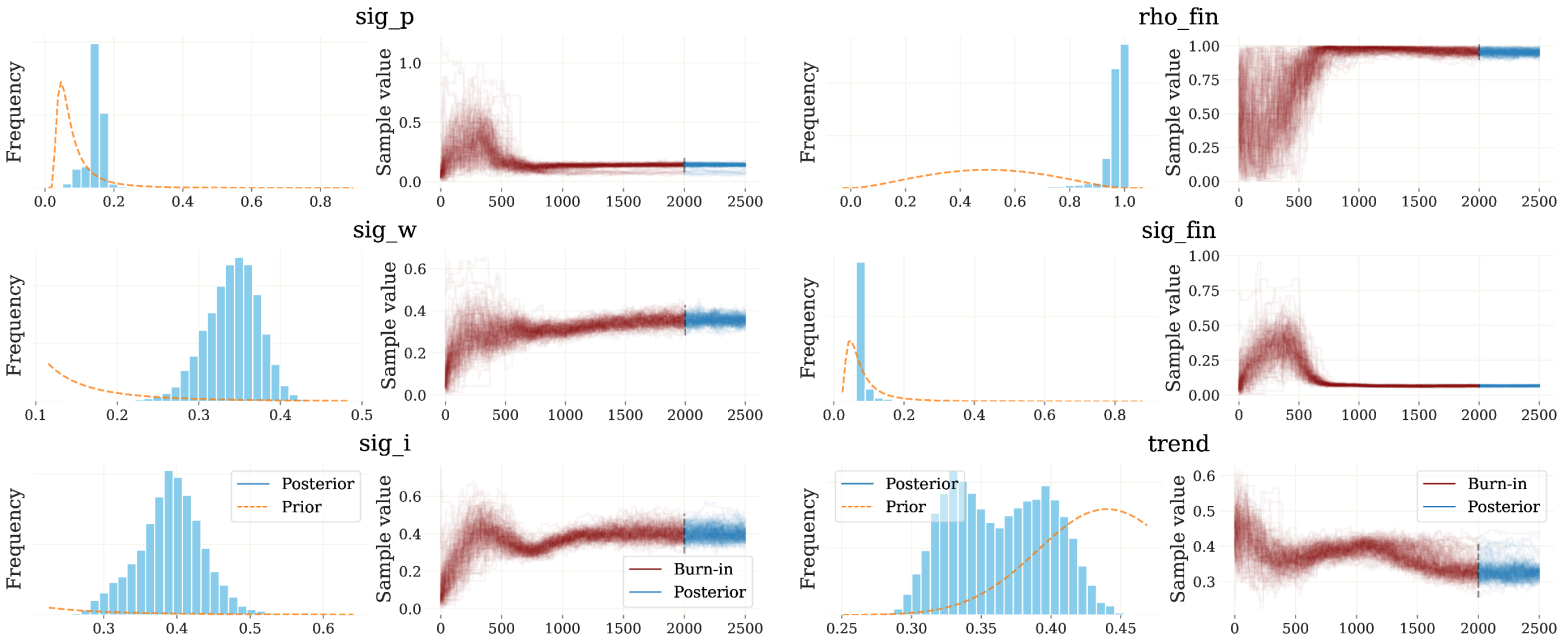

Figure E.21: Traceplots of the 200 DIME chains for selected parameters. Estimation of the FRANK model. The left panel shows a KDE of the parameter distribution. The right displays the trace of each of the chains over time.

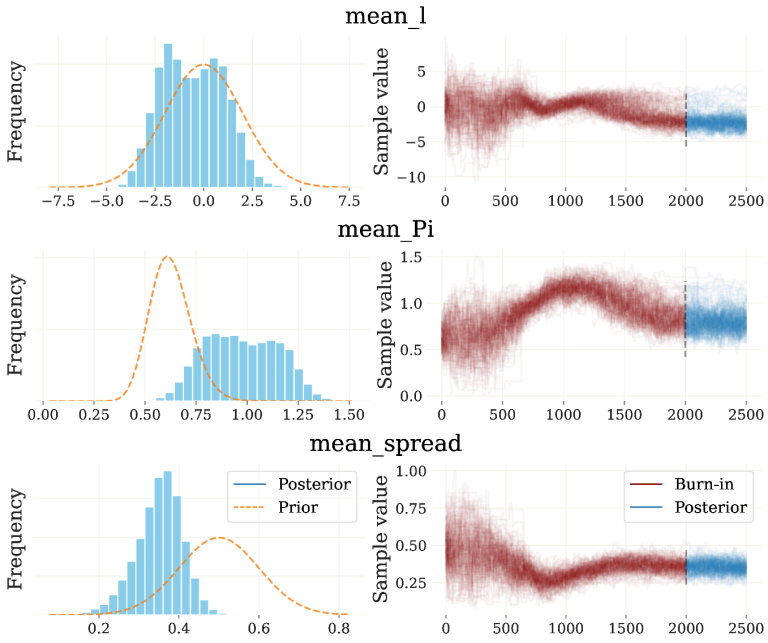

Figure E.22: Traceplots of the 200 DIME chains for selected parameters. Estimation of the FRANK model. The left panel shows a KDE of the parameter distribution. The right displays the trace of each of the chains over time.